Matematisk-fysiske Meddelelser
udgivet af
Det Kongelige Danske Videnskabernes Selskab
Bind **32**, nr. 12

Mat. Fys. Medd. Dan. Vid. Selsk. **32**, no. 12 (1960)

HALF LIVES OF FIRST EXCITED STATES OF EVEN NUCLEI OF Em, Ra, Th, U, and Pu

BY

R. E. BELL, S. BJØRNHOLM, AND J. C. SEVERIENS

København 1960
i kommission hos Ejnar Munksgaard

CONTENTS

Synopsis

The half lives of the first excited states of eighteen even nuclei of Em, Ra, Th, U, and Pu have been measured, and an upper limit has been set for a nineteenth. The measurements were made by the delayed coincidence method, using a fast time-to-amplitude converter. The experimental half lives were all found to lie between 1.5 and 7.6×10^{-10} sec. The results are used to calculate reduced transition probabilities, quadrupole moments, and deformation parameters for the nuclei concerned. Comparisons are made between these values and recent theoretical calculations. Agreement within 10 % or less is found. As by-products of the present work, upper limits have been set for the half lives of two excited states in Th^{230} and U^{233}, and the calculated $E2$ conversion coefficients of Rose have been verified within about 15 % for this region of Z and energy.

Printed in Denmark
Bianco Lunos Bogtrykkeri A-S

1. Introduction

The measurements to be described here constitute an experimental survey of the half lives of first excited states of even nuclei between Em^{218} and Pu^{240}. This part of the periodic table is one of the two most prominent regions showing large stable deformations of the nuclei, the other one being the rare earth region extending roughly from samarium to wolfram. The even nuclei in these regions show the typical spectrum of rotation of a deformed axially symmetric structure, viz., a band of energy levels of character $0+, 2+, 4+, \ldots$ having energies closely given by

$$E = \frac{\hbar^2}{2\Im} I(I+1). \tag{1}$$

Equation (1) and the other equations to follow are conveniently collected in the review paper of ALDER *et al.*[1]). From the observation of these energy levels, the effective moment of inertia, $\Im$, is at once known. The actual amount of distortion of the nucleus cannot be deduced from $\Im$, however, without more detailed knowledge of the nuclear motion.

Experimentally, the nuclear quadrupole deformation is derived from measurements of the pure electric quadrupole transition rate between adjacent levels in the rotational band, usually between the $0+$ ground state and the $2+$ first excited state. This rate may be measured either by measuring the cross section for Coulomb excitation of the $2+$ state from the $0+$ ground state, or by measuring the half life, $T_{1/2}$, of the reverse gamma transition $(2+ \to 0+)$ in a radioactive source. Given this half life, the rate of gamma ray emission $(2+ \to 0+)$ is $T(E2;\ 2 \to 0) = (ln2)\ [(1+\alpha)\ T_{1/2}]^{-1}$, where α is the total conversion coefficient; then

$$T(E2;\ 2 \to 0) = \frac{4\pi}{75} \frac{1}{\hbar} \left(\frac{E}{\hbar c}\right)^5 B(E2;\ 2 \to 0), \tag{2}$$

where $B(E2;\ 2 \to 0)$ is the reduced transition probability. The quantity found in Coulomb excitation experiments is

$$B(E2; 0 \to 2) = 5\, B(E2; 2 \to 0) \tag{3}$$

on grounds of statistical weight. If this transition probability is due to rotation of a deformed nucleus of intrinsic quadrupole moment Q_0, we may find Q_0 from

$$B(E2; 0 \to 2) = 5\, (16\pi)^{-1} e^2 Q_0^2. \tag{4}$$

If the nuclear shape is spheroidal, we may use the distortion parameter β given by

$$\beta = \frac{4}{3}\left(\frac{\pi}{5}\right)^{1/2} \frac{\Delta R}{R_0} = 1.06 \frac{\Delta R}{R_0},$$

where ΔR is the difference between the major and minor semi-axes, and R_0 is the mean radius. The value of β may now be calculated from Q_0 by the use of

$$Q_0 = 3(5\pi)^{-1/2} Z R_0^2 \beta (1 + 0.16\,\beta + \ldots). \tag{5}$$

Thus, an experimental half life leads directly to an experimental Q_0 and β for the nucleus in question.

The nuclear moment of inertia depends on the structure of the intrinsic nucleonic motion.

If the nucleons in the rotating nuclear field behaved as completely independent particles, the effective moment of inertia would be approximately that corresponding to rigid rotation,

$$\Im_{\text{rig}} = \frac{2}{5} \text{AMR}_0^2 (1 + 0.31\,\beta + \ldots), \tag{6}$$

where A is the atomic number and M the nucleon mass. Residual interactions between the nucleons in addition to the interaction included in the average binding field give rise to correlations in the intrinsic motion, which reduce the moment.

In the other extreme, if the residual interaction were so strong as to break down the independent-particle motion completely, the effective moment of inertia would approach the hydrodynamic value, equivalent to a wave travelling irrotationally on the surface of a liquid drop. In that case,

$$\Im_{\text{irrot}} = \frac{2}{5} \text{AMR}_0^2 \beta^2 (0.89 + 0\,(\beta^2)). \tag{7}$$

In fact, the moments of inertia are found to lie between the extremes, their actual values furnishing information on the strength of the residual

interactions between nucleons. Recently, methods have been developed for incorporating effects of these residual interactions (the pairing correlations). It has thereby become possible to make a more detailed comparison between theory and experiment than was previously feasible. This question will be raised again in the discussion section of this paper.

Before the present work was done, transition probabilities had been well studied in the rare earth region both by Coulomb excitation and by lifetime measurements, while comparatively little was known of the heavy element region. Among the heavy even nuclides, half lives had been measured for the first excited states of Em^{220}, Ra^{224}, and Ra^{226}, and Coulomb excitation measurements existed for Th^{232} and U^{238}. Details of these existing measurements are given later, in the experimental section of this paper. (The nuclides just mentioned are included in the present study, in one case with a different result (Em^{220})). The reason for the lack of lifetime data is that the experimental half lives lie close to the limit of present day delayed coincidence techniques, around 10^{-10} sec for the low energies involved. The reason for the lack of Coulomb excitation data is that all the nuclides concerned are radioactive, and target preparation becomes difficult or impossible. Four Coulomb excitation results are available for odd nuclides in this region (U^{233}, U^{235}, Np^{237}, Pu^{239}).[1] We have avoided odd nuclides in this work for two reasons. First, the rotational transitions in odd nuclei contain strong $M1$ admixtures with the $E2$ part, thus shortening the experimental half lives to be measured, and rendering the interpretation less definite. Second, odd nuclei display effective moments of inertia 15 to 50 % greater than their even neighbours, owing to the presence of the extra odd particle.[1] They are therefore not immediately comparable with even nuclei.

2. Experiments and Results

The apparatus used for the half life measurements was a fast time-to-amplitude converter generally similar to that described by GREEN and BELL[2], but with a number of modifications. Some of these are described briefly in a paper by BELL and JØRGENSEN[3]. The circuit employed RCA-6342A photomultipliers and organic scintillators, often made of NE 102 plastic. In a typical measurement, an alpha emitter having a branch feeding the desired excited state was sandwiched between two organic scintillators, one detecting the alpha particles and the other the conversion electrons of the transition from the excited state to the ground state. The time-to-amplitude

converter then produces an output pulse spectrum that represents the distribution of time delays between the preceding alpha particles and the subsequent conversion electrons. (Occasionally, the preceding radiation was beta or gamma rays rather than alpha particles.) From this spectrum, observed with a 100 channel pulse analyzer, the half life of the excited state can be read off. In every case, the instrumental time resolution was good enough to allow the half life to be found directly from the logarithmic slope of the recorded time distribution.

The calibration of the pulse amplitude spectrum in terms of time is done by lengthening the cable delay from one of the counters by a measured amount, and observing the shift of the distribution along the amplitude scale. A standard error of 3 % has been adopted to take account of any errors in this procedure. The standard error in any particular measurement reported here varies with the circumstances, but the 3 % just mentioned forms a lower limit.

The individual sections to follow are arranged approximately in the chronological order in which the measurements were performed. All statements about the radioactive properties of the various sources are taken from standard compilations, usually STROMINGER, HOLLANDER, and SEABORG[4], except where separate references are given. Chemical and physical procedures for the preparation and mounting of the sources are given in each case.

(a) Th^{226} (72 keV), Ra^{222} (111 keV), Em^{218} (325 keV)

The measurements on these three excited states were made using a single source of U^{230} and its descendants in equilibrium. The procedures will be described in detail, both because they are typical of those used in all the other cases, and because the U^{230} source is the most complex one used in this study.

The activity was obtained from a source of Pa^{230} (18 *d*), which decays to U^{230} (21 *d*) by a 15 % beta branch. The Pa^{230} had been made by a 65 MeV, 4 μamp-hour proton bombardment on 0.3 g of thorium metal.* The protactinium was separated from thorium and fission products by anion exchange. First it was absorbed on Dowex 1 from a 12 N HCl solution, allowing the thorium to pass through the ion exchange column. The protactinium was then eluted with a 2 N HCl solution. The procedure was repeated using

* We are indebted to Ing. ÅKE SVANHEDEN and the crew of the cyclotron of The GUSTAF WERNERS INSTITUTE, Uppsala, for carrying out the bombardment.

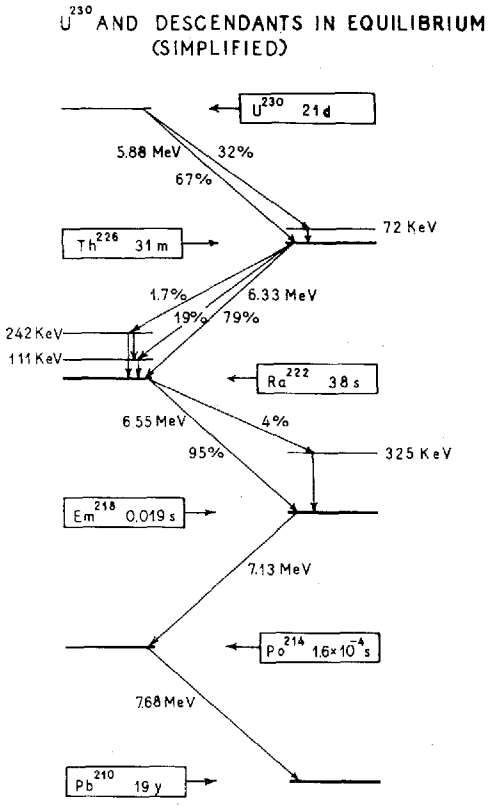

Fig. 1. A simplified decay scheme of U^{230} and its descendants. All branches of less than 1% intensity are omitted.

a solution 9 N in HCl and 0.006 N in HF as eluant. Finally, a third cycle was made using the former eluant. The protactinium sample contained all the isotopes from Pa^{228} to Pa^{233}, but only Pa^{230} gives rise to a uranium daughter of any appreciable activity. After letting U^{230} grow in for about three weeks, a separation of protactinium and uranium was performed. The activity was again absorbed on Dowex 1 from 12 N HCl and eluted with the above mentioned HCl-HF mixture, uranium remaining on the column. U^{230} was eluted with a 0.5 N HCl solution and the purification cycle was repeated. After evaporation of the HCl solution the source was ready. No visible material was present, as should also be expected.

U^{230} is the parent of a chain of five successive alpha decays, ending (for our purposes) with 19 year Pb^{210}. A simplified decay scheme of this

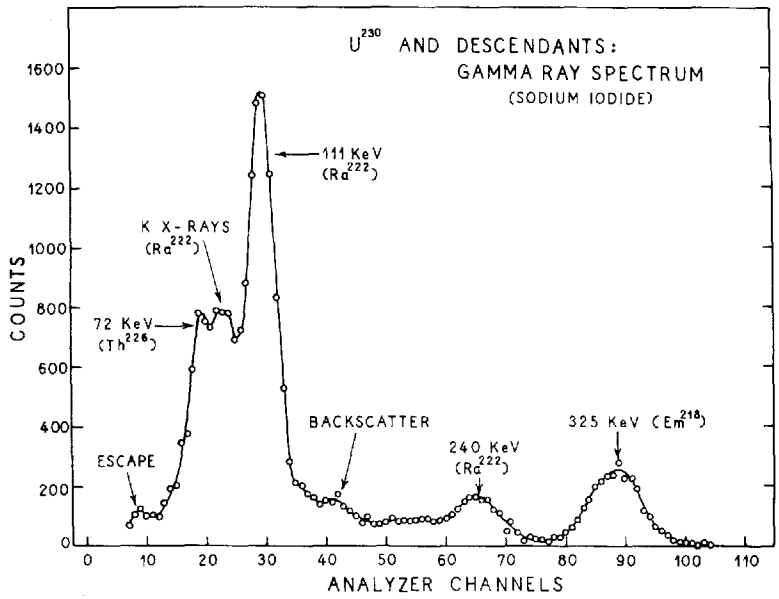

Fig. 2. The gamma ray spectrum of U^{230} and its descendants, seen in a sodium iodide scintillation counter.

chain is shown in fig. 1, in which all branches of less than 1% intensity have been omitted. All the observations made on our U^{230} source are consistent with this scheme in energy and intensity. Before the U^{230} source was finally mounted, its X- and gamma-rays were observed with a sodium iodide counter. The result, fig. 2, shows radiations that are easily identified from fig. 1, and no others. Fig. 2 shows that the source is free of Pa^{230}, which has strong K X-rays and high energy gamma rays. The fact that the 325 keV gamma ray is the highest-energy one of appreciable intensity is used later in the measurement of Em^{218}.

The U^{230} activity was deposited on a 0.020 mg/cm^2 plastic foil and covered with a 0.15 mg/cm^2 aluminium foil. This pair of foils was sandwiched between two discs of NE-102 plastic phosphor, each 20 mm in diameter and 2 mm thick, which in turn were coupled to two RCA-6342A photomultipliers. The whole assembly constituted a pair of independent 2π counters working on the same source. The total source strength in all five members of the decay chain was about 3×10^4 disintegrations per second.

The pulse height spectrum of one of the 2π counters is shown in fig. 3. The spectrum is dominated by a broad peak at about 250 keV equivalent

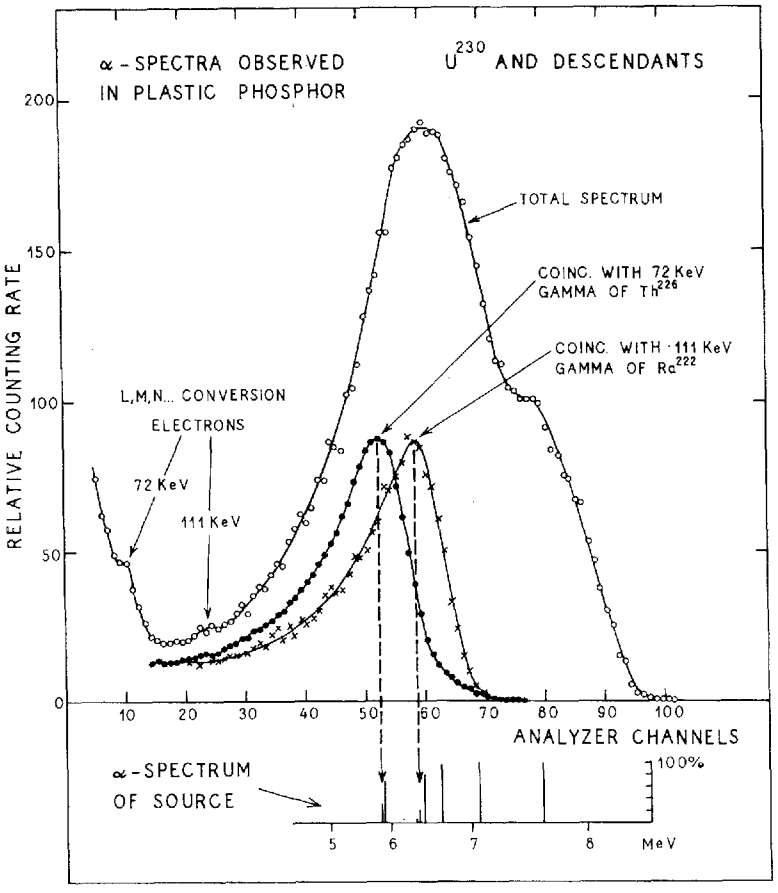

Fig. 3. The pulse height spectrum of U^{230} and its descendants, seen in a 2 mm thick plastic phosphor. Two coincidence alpha spectra are also shown. A separate scale at the bottom shows the alpha energy scale.

electron energy, caused by the ≈6 MeV alpha particles. This peak shows only faint signs of resolution into its component alpha energies. At lower energies there are slight indications of the LMN . . . conversion peaks of the 72 keV and 111 keV radiations of Th^{226} and Ra^{222}, respectively. (The coincident alpha peaks in fig. 3 are discussed later.)

A pulse height window was set to cover the broad alpha peak in fig. 3, and was left there for all the subsequent observations. The counter so arranged may now be designated the alpha counter. The spectrum of pulses from the other scintillation counter (the electron counter) coincident

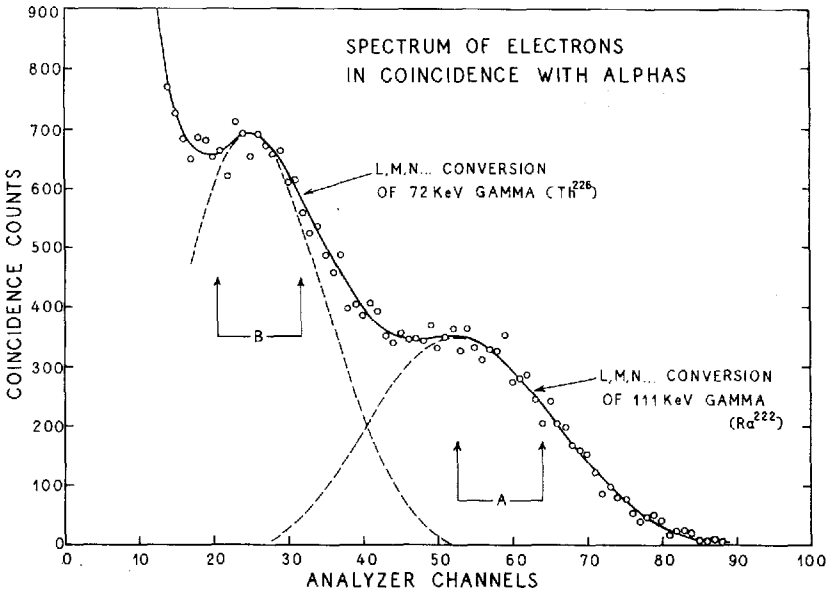

Fig. 4. The pulse height spectrum in a 2 mm plastic phosphor of conversion electrons in coincidence with alpha particles, for U^{230} and its descendants. The dashed curves are illustrative only. The two pulse height windows A and B were used in the half life measurements.

with these alpha pulses is shown in fig. 4. Two broad peaks appear, corresponding to the LMN . . . conversion of the 72 and 111 keV transitions of Th^{226} and Ra^{222}, respectively. Broken lines in fig. 4 indicate in a rough way how the two peaks may be separated.

The two pulse height windows A and B in fig. 4 enable us to detect the 111 and 72 keV transitions almost independently. For verification of this fact, we refer again to fig. 3. Here we have plotted the spectra of alpha pulses coincident with the 72 and 111 keV transitions. The two alpha peaks so revealed are clearly separate. It still cannot be excluded that some pulses from the 111 keV transition are mixed with those from the 72 keV transition, perhaps to the extent of a few percent. Fortunately the two transitions turn out to have half lives only about 30 % apart; the possible admixture effect has been taken into account by assigning fairly generous standard errors to the measured half lives.

The two coincident alpha peaks, plus the partially resolved high energy alpha group in the singles spectrum, allow us to attach a rough scale of alpha energies at the bottom of fig. 3, with the alpha spectrum of the source. The scale is non-linear, as expected for a plastic phosphor.

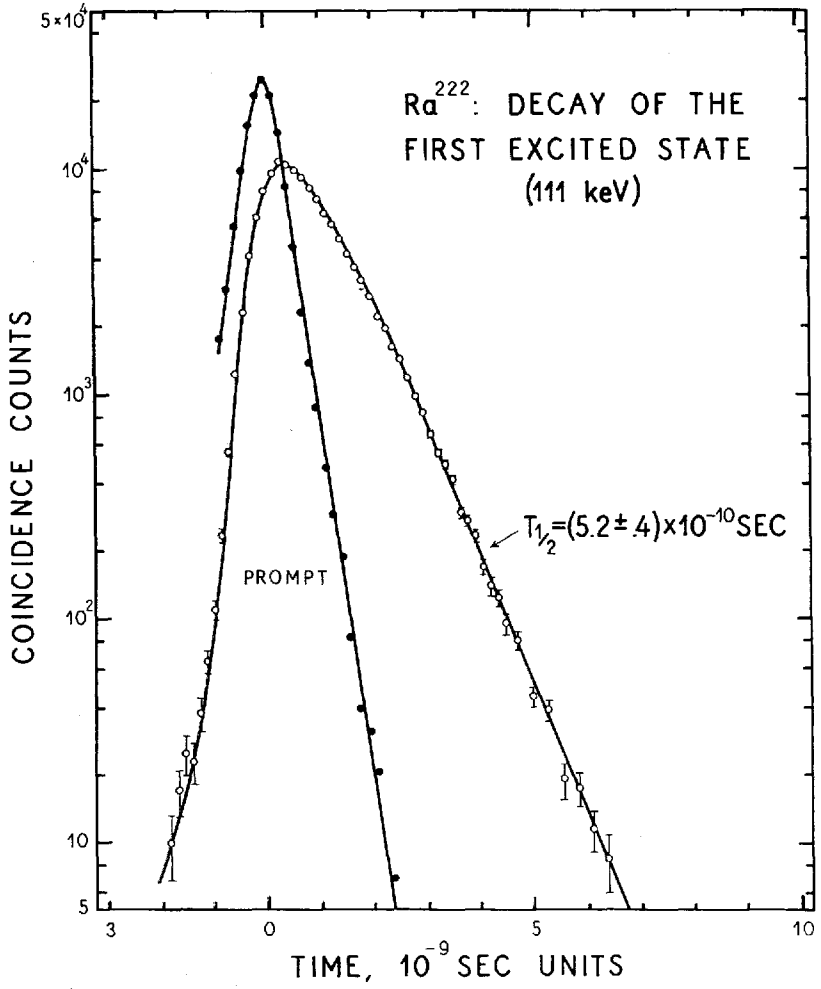

Fig. 5. The time analysis of the coincidences between alpha particles and conversion electrons of the 111 kev radiation of Ra^{222}. A prompt resolution curve is shown for illustrative purposes.

The time analysis of coincidences between alpha particles and the 111 keV radiation of Ra^{222} (pulse height window A, fig. 4) is shown in fig. 5. The half life read from this curve is $(5.2 \pm 0.4) \times 10^{-10}$ sec. The prompt resolution curve shown in fig. 5 is included, for illustrative purposes only, to show that the slope of the 111 keV curve is real and not instrumental. This prompt curve was made by partially removing the aluminium foil separating the alpha counter from the electron counter, so that a little light from each alpha

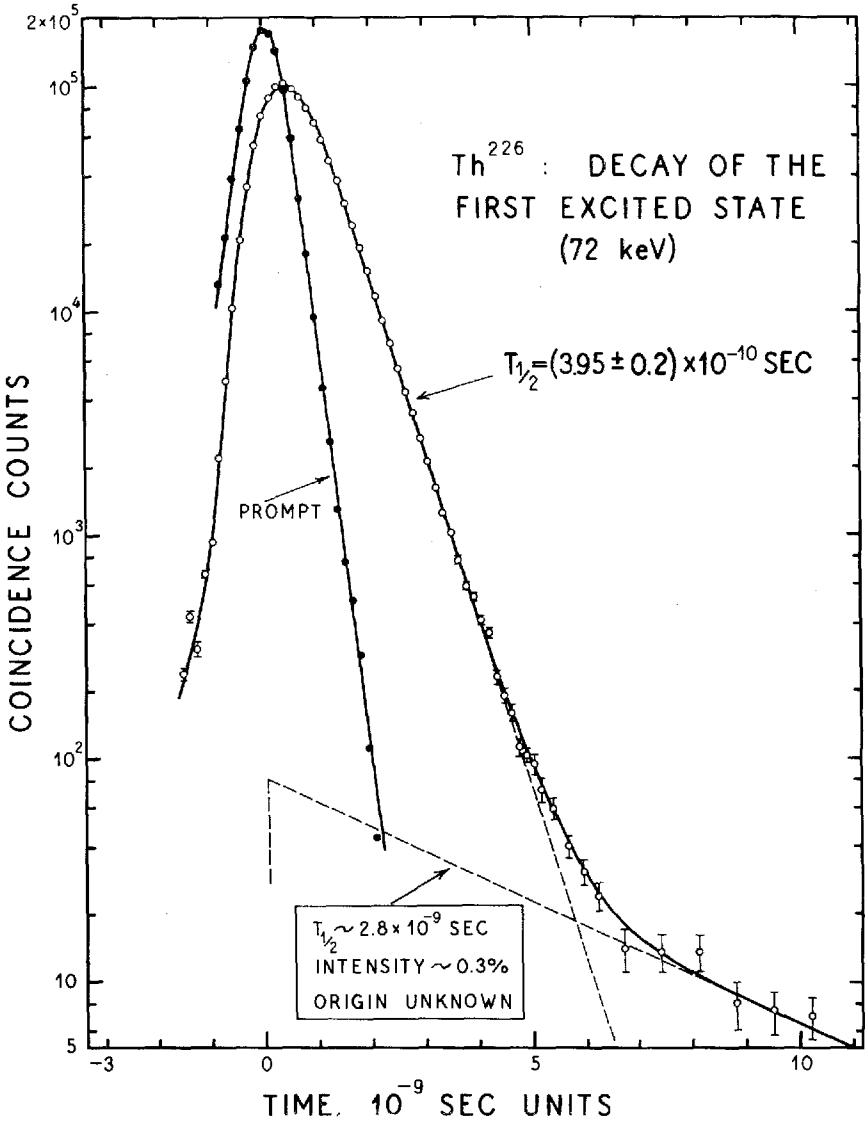

Fig. 6. The time analysis of the decay of the first excited state of Th^{226}. A weak component of longer half life has been subtracted. A prompt resolution curve is shown for illustrative purposes.

scintillation could enter the electron counter. In this way every alpha pulse is made to yield a true coincidence, with no change of discriminator settings. (No claim is made that this procedure yields a highly accurate prompt

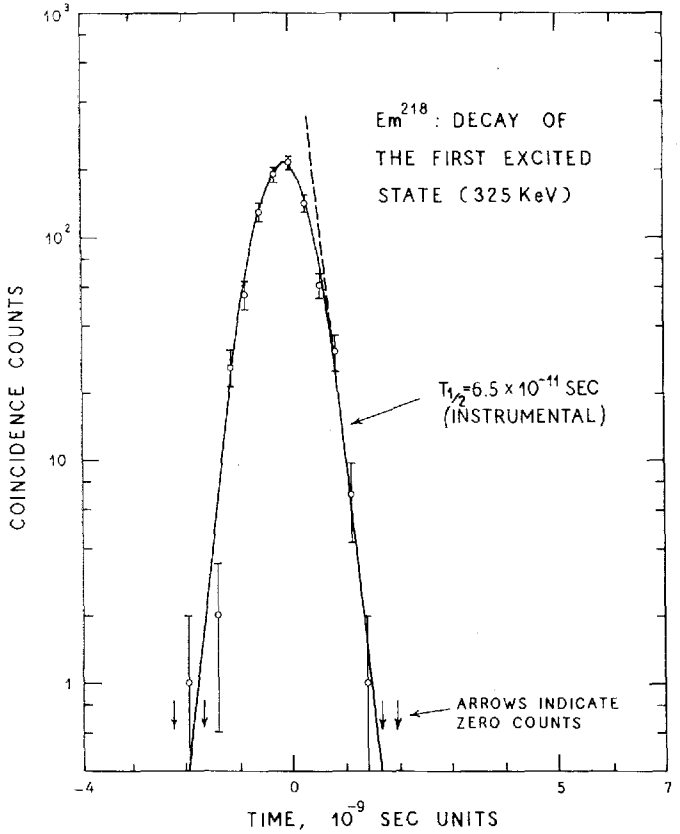

Fig. 7. The time analysis of the decay of the first excited state of Em^{218}. No half life longer than 6.5×10^{-11} sec was observed, and the experimental limit has been taken as 8×10^{-11} sec.

resolution curve; an accurate curve should be somewhat narrower and steeper than the one shown.)

The time analysis of the 72 keV radiation of Th^{226} (pulse height window *B*, fig. 4) is shown in fig. 6. The half life read from this curve is $(3.95 \pm 0.2) \times 10^{-10}$ sec. A prompt curve is also shown, made in the same way as that described in the previous paragraph. At the foot of the 72 keV curve there appears a weak component (total intensity 0.3 % of the 72 keV curve) with a half life of about 2.8×10^{-9} sec. This component is so weak that its presence does not interfere with the accuracy of reading the main half life. Its origin could be in any one of several very weak radiations not shown in the decay scheme of fig. 1, or in some minor impurity in the source. We can

speculate that its energy must be low, because it appears in the 72 keV curve, but not in the 111 keV curve. It was not investigated further.

The final observation on the U^{230} chain concerned the 325 keV first excited state of Em^{218}. For this measurement the electron counting crystal was removed and a 15 mm thick diphenylacetylene (DPA) gamma counter was put in place of it, shielded by enough aluminium to stop all electrons. By the use of auxiliary radioactive sources, this counter was biased to respond only to gamma rays above 250 keV. Reference to fig. 2 shows that this counter then detects only the 325 keV gamma ray of Em^{218}. The time analysis for this radiation is given in fig. 7. The curve shows only the instrumental resolution of the apparatus, with a slope on its right-hand edge corresponding to $T_{\frac{1}{2}} = 6.5 \times 10^{-11}$ sec. We may therefore state conservatively that the half life of the 325 keV level of Em^{218} is less than 8×10^{-11} second.

(b) Th^{230} (53 keV), U^{230} (51.7 keV)

Pa^{230} (18 *d*) decays both by electron capture to Th^{230} (85 %) and by beta emission to U^{230} (15 %). The electron capture decay to Th^{230} is accompanied by plentiful high energy gamma rays (400 keV to 950 keV), many of which feed the first excited state at 53 keV. The beta decay to U^{230} has no high energy gamma rays. Thus, coincidences between high energy gamma rays and low energy conversion electrons are due solely to the first excited state of Th^{230}. As we shall see, no such simple selection scheme applies to U^{230}, and the results for this nucleus are of lower accuracy.

The source of mixed protactinium activities mentioned in the preceding section (a) was used in the present measurement. The half lives of the protactinium isotopes are such that after a few weeks only Pa^{230}, and possibly Pa^{233} (27 *d*), remain in the source. Under the bombarding conditions mentioned (65 Mev protons), the cross section for the formation of Pa^{230} largely exceeds that of Pa^{233}, therefore the activity will be relatively pure Pa^{230}. The protactinium fraction from the protactinium-uranium separation already described could thus be used as source of Pa^{230}. The lifetime measurements were performed within one day after chemical separation, to avoid complications from the growth of U^{230} (21 *d*) and its daughters.

In order to estimate the amount of Pa^{233} present in the source, a comparison was made between the sodium iodide gamma spectrum of our Pa^{230} source and that of a source of pure Pa^{233} of roughly known strength. No Pa^{233} was detected, and an upper limit of 10 % could be set for the abundance of Pa^{233} in the Pa^{230} source.

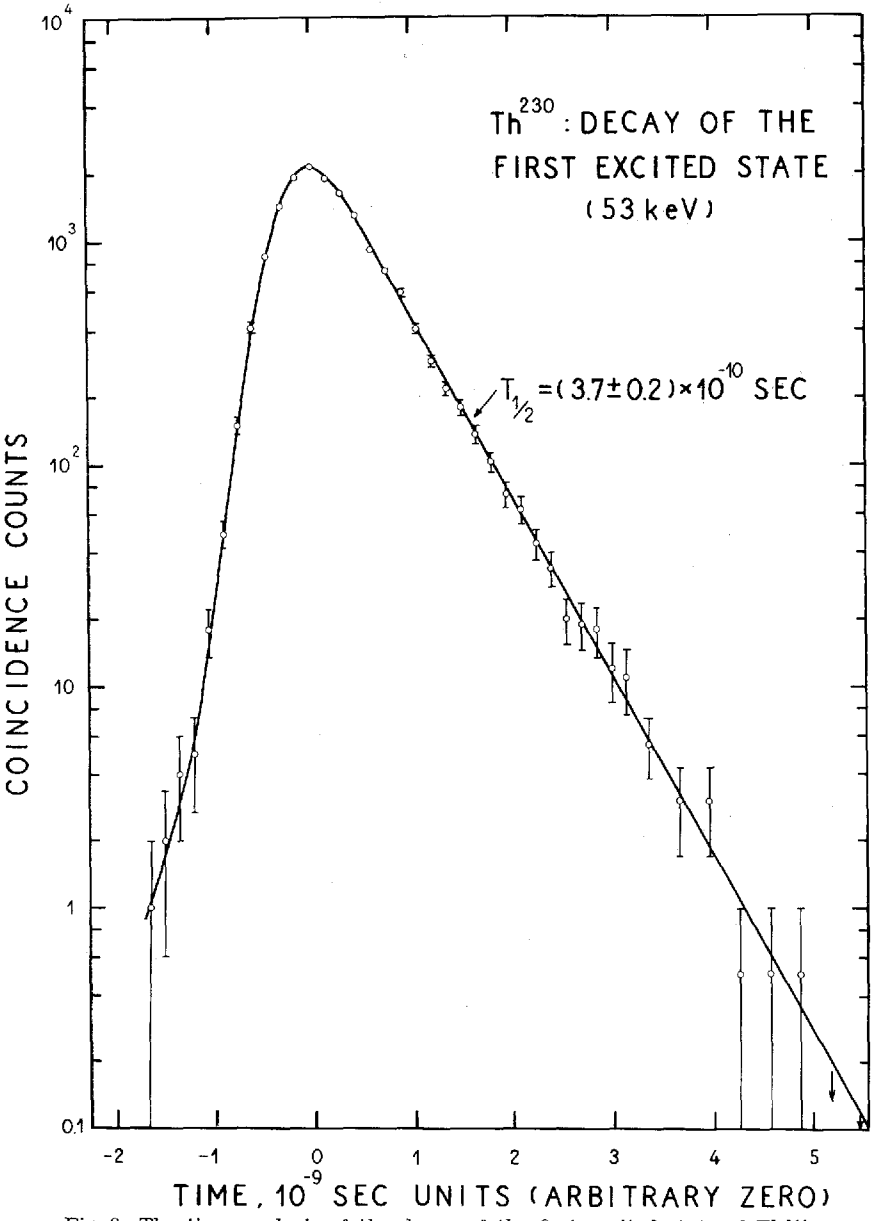

Fig. 8. The time analysis of the decay of the first excited state of Th^{230}.

As a control experiment, a lifetime measurement was made on a Pa^{233} source in the same manner as for the Pa^{230} source, described below. The yield of coincidences was small, and no half life in excess of 10^{-10} sec was present. We are thus assured that the Pa^{230} results are not disturbed by the presence of a possible small impurity of Pa^{233}. A second control experiment consisted of a gamma-gamma coincidence experiment on the Pa^{230} source before it was finally mounted, which showed that the intermediate states between high energy gamma rays in Th^{230} have half lives less than 10^{-10} sec. As a result of these control experiments we can say definitely that the 508 keV level of Th^{230} and the 313 keV level of U^{233} have half lives less than 10^{-10} sec.

For the measurement of the Th^{230} 53 keV half life, the source of Pa^{230} was mounted on a 2 mm thick plastic phosphor. A 15 mm thick DPA gamma counter was placed next to this source, and adjusted to accept pulses from gamma rays above 600 keV, i.e., principally the ≈ 900 keV gamma rays feeding the 53 keV state. The low energy electrons in the plastic counter in coincidence with these gamma rays showed a clean peak due to LMN... conversion electrons of the 53 keV transition, with even a hint of resolution of the MN... peak. A broad pulse height window was placed on this peak, and the coincidence resolution curve was measured. The result, fig. 8, shows a clean decay with a half life of $(3.7 \pm 0.2) \times 10^{-10}$ sec for the 53 keV state.

The measurement of the half life of the 51.7 keV excited state of U^{230} is more difficult. The preceding radiation is the weak beta decay branch of Pa^{230}, with end point energy 360 keV, but this spectrum is overlain by conversion lines from the stronger electron capture branch. The gamma counter mentioned in the preceding paragraph was removed and a 2 mm plastic electron counter was substituted for it. The pulse spectrum of this counter showed evidence of discrete groups (conversion lines) in addition to the desired continuum, but the resolution was of course not good enough to enable us to choose any pulse height region that avoided the conversion lines. Under these conditions, the resolution curves will show a mixture of the desired U^{230} lifetime and the unwanted Th^{230} lifetime already measured. Several curves were measured with different biases on the beta counter (the bias on the original conversion electron counter remaining fixed), and the one with the best ratio of U^{230} effect to Th^{230} effect is shown in fig. 9. The curve was purposely run to a very high statistical accuracy; it shows the expected mixture of the known half life of the Th^{230} excited state, 3.7×10^{-10} sec, and a shorter half life due to the U^{230} excited state. The resolution of this decay curve into its two components would be very difficult if it were not for the fact that we already know the longer half life accurately. The

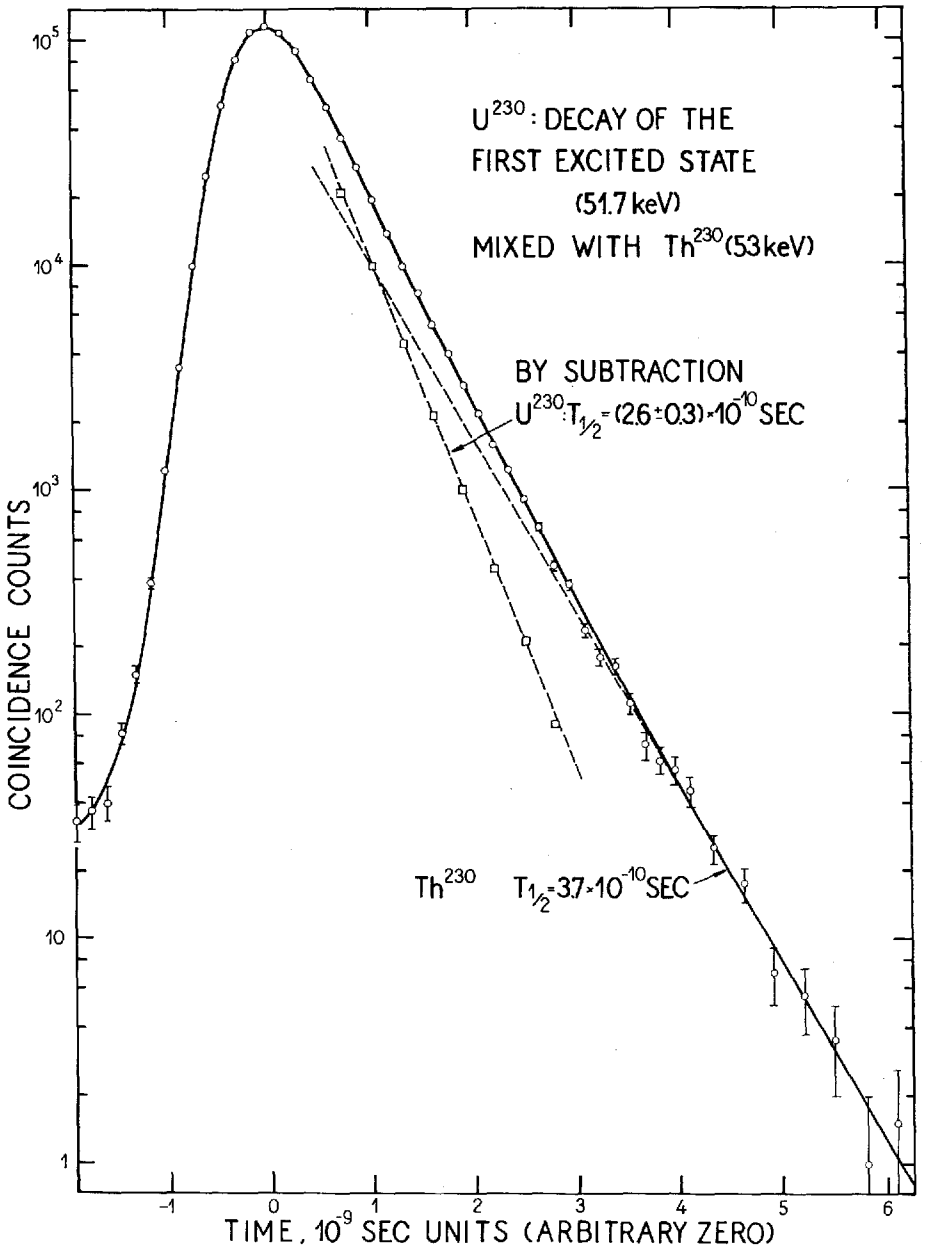

Fig. 9. The time analysis of the decay of the first excited state of U^{230}. The subtraction shown is assisted by prior knowledge of the longer half life (see section (b) and fig. 8).

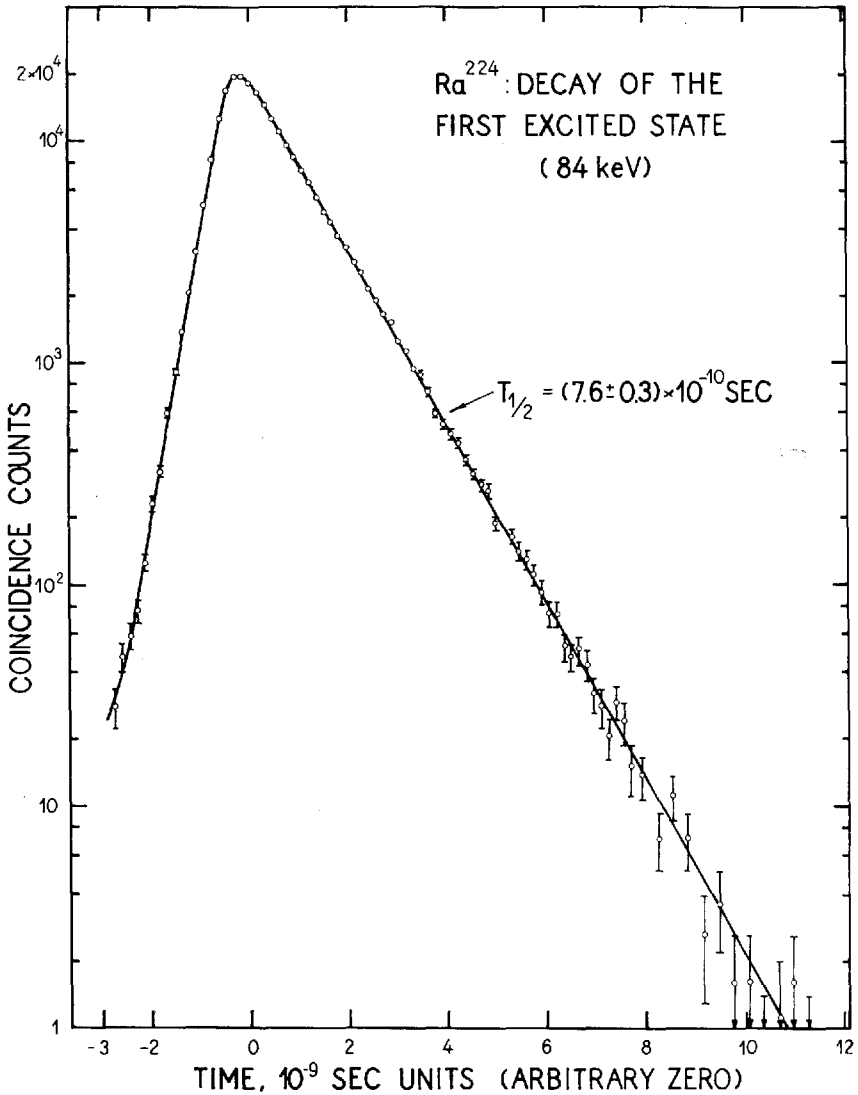

Fig. 10. The time analysis of the decay of the first excited state of Ra^{224}.

subtraction indicated by broken lines in fig. 9 yields a half life of 2.6×10^{-10} sec for the first excited state of U^{230}. The error to be quoted in this value is to some extent a matter of judgement. Adjusting the position of the subtracted component (Th^{230}) causes a variation in the result for the half life

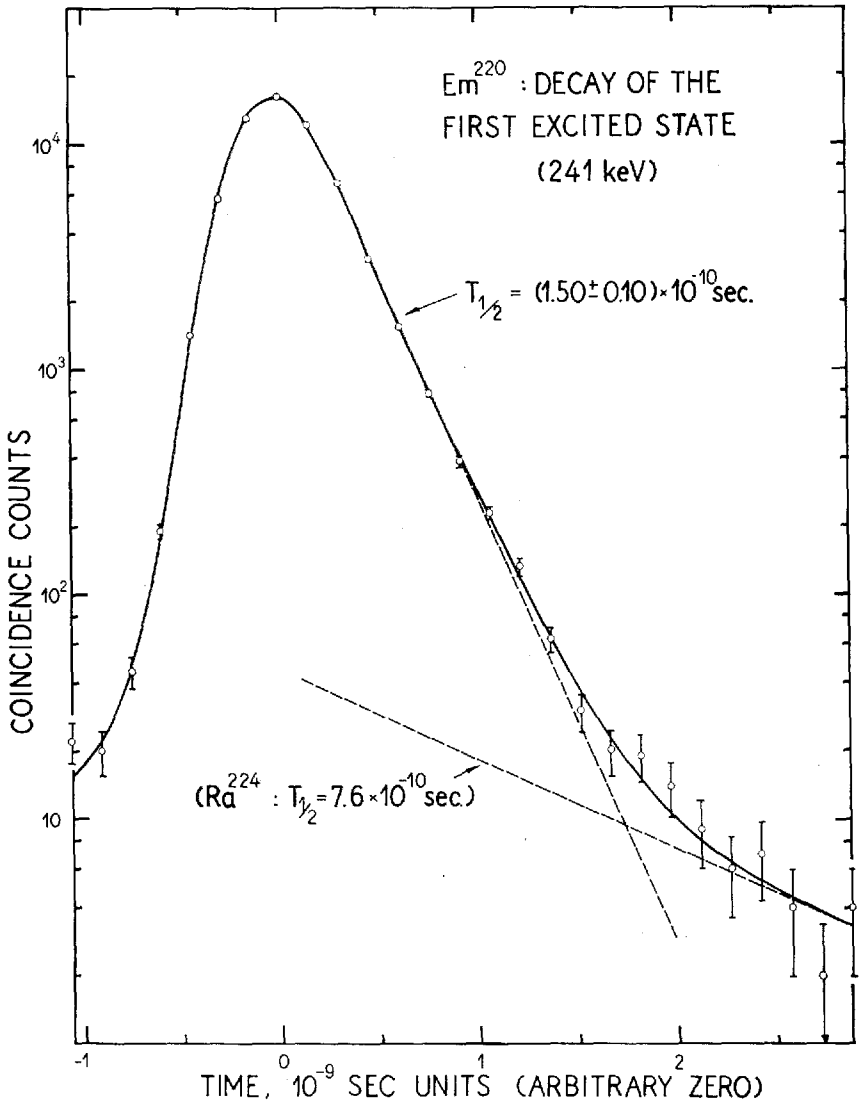

Fig. 11. The time analysis of the decay of the first excited state of Em^{220}. A small contribution from Ra^{224} has been subtracted.

of the remainder (U^{230}); we take, as the limits of our standard error, the half lives outside which the remainder curve shows a distinct curvature. In this way we arrive at the value $(2.6 \pm 0.3) \times 10^{-10}$ sec. The fractional error quoted is larger than that of most of the other measurements in this series.

It would be worth while to have a better value for this half life. Since Pa^{230} is the only radioactivity that populates the excited state of U^{230} to an appreciable extent, the sole way to observe the U^{230} decay alone is to use magnetic selection to resolve the radiations leading to U^{230} from the stronger ones leading to Th^{230}. We were not equipped to do this at the time the source was available.

(c) Ra^{224} (84 keV)

The half life of this excited state has been measured previously by SIEKMAN and DE WAARD[5] both by the delayed coincidence method (centroid shift) and by the recoil method (Doppler shift of conversion line). Their results were $T_{\frac{1}{2}} = (7.5 \pm 1.5) \times 10^{-10}$ sec and $T_{\frac{1}{2}} = (7.0 \pm 1.0) \times 10^{-10}$ sec, respectively. SEVERIENS and RICHTER[6] have found a value $T_{\frac{1}{2}} = (6.0 \pm 1.6) \times 10^{-10}$ sec by another recoil method. VARTAPÉTIAN[7] finds $T_{\frac{1}{2}} = (8.4 \pm 0.7) \times 10^{-10}$ sec by delayed coincidences, again using the centroid-shift method.

The present measurement was made using a source of Th^{228} (RdTh, 1.9 *y*), an alpha emitter having a 28 % branch to the 84 keV state of Ra^{224}. The source was prepared from a sample of Th^{228} in equilibrium with its daughter activities. Of these Ra^{224} (3.6 *d*) and Pb^{212} (10 *h*) have the longest half lives. Once these two activities are removed, the remaining daughters soon die away. In order to prepare the Th^{228} free of radium and lead, the activity was absorbed on a cation exchange column. The column was eluted with 7 N HCl, which removed lead and radium. Thorium was eluted with a 1 M ammonium lactate buffer of pH ≈ 3.4. The volume of the resin filling of the ion exchange column was chosen to be very small (15 μl). The purified thorium activity was therefore present in a very small volume, < 5 μl, which was spread over an area of one square centimeter and dried. In this way a source thickness much less than 0.5 mg/cm^2 was assured.

All the measurements on the half life of the 84 keV state of Ra^{224} were completed within 10 hours of the chemical separation, in order to minimize complications arising from the growth of the 3.6 day Ra^{224} and its descendants. The source material was deposited on the surface of a piece of 10 mg/cm^2 plastic phosphor (NE 102), so that only alpha particles could produce large pulses with appreciable probability. The conversion electron counter was a 2 mm thick plastic phosphor separated from the alpha counter by a 0.15 mg/cm^2 aluminium foil. The spectrum of electron pulses in coincidence with alpha pulses showed a peak due to LMN... conversion of the 84 keV gamma ray, and a pulse height window was set on this peak.

The time analysis of the resulting coincidences is shown in fig. 10, and yields the result $T_{\frac{1}{2}} = (7.6 \pm 0.3) \times 10^{-10}$ sec for the 84 keV state of Ra^{224}. Within their errors, all the previously measured values agree with this one.

(d) Em^{220} (241 keV)

The source of Th^{228} used for the measurement of the Ra^{224} excited state (see the preceding section (c)) was allowed to stand for two days so as to accumulate an appreciable amount of the 3.6 *d* Ra^{224} daughter and its descendants. Ra^{224} is an alpha emitter having a 5 % branch to the 241 keV excited state of Em^{220}. For the measurement of this state, the alpha counter was left unchanged, and the electron counter was covered with 11 mg/cm^2 of aluminium, sufficient to stop all alpha particles and all electrons of energy lower than about 90 keV. The pulse spectrum of the electron counter in coincidence with alpha particles showed two clearly resolved peaks corresponding to K and LMN... conversion of the 241 keV gamma ray. The K/LMN... ratio was about 0.7, in agreement with expectation for an $E2$ gamma ray of this energy. A pulse height window was set on the LMN... peak, and the time analysis of the resulting coincidences is shown in fig. 11. The curve shows a decay with $T_{\frac{1}{2}} = (1.50 \pm 0.10) \times 10^{-10}$ sec, followed by a weak tail having a half life near the value 7.6×10^{-10} sec appropriate to the 84 keV level of Ra^{224}, already measured. The tail is presumably due to a few 84 keV gamma rays dissipating their full energy in the electron counter. The presence of this tail does not in any case interfere with the evaluation of the main half life in fig. 11. The further descendants of Ra^{224}, extending to Pb^{208}, do not include any alpha emitters having appreciable branching to excited states with energies high enough to register in the electron counter. Two other runs, of lower statistical accuracy, were made on this excited state. In one of them, the pulse height window in the electron counter was moved from the LMN... peak to the K peak. In the other, the electron counter was replaced by a 15 mm thick DPA gamma counter biased to detect the 241 keV gamma rays. In both cases, the result was in agreement with that given above. A final check was made to ensure that the half life found was not dangerously close to the limit of resolution of the apparatus. For this purpose, the thin alpha counter was removed and replaced by a 2 mm plastic phosphor. The counters were reassembled and a 5 μC source of Na^{22} was placed nearby. There was enough scattering between the counters of secondary electrons produced by the gamma radiation from this source

to give a small prompt coincidence counting rate, with the same biases on the counters as before. The resulting resolution curve had a slope on its right hand side corresponding to $T_{\frac{1}{2}} = 7.5 \times 10^{-11}$ sec, about as expected; thus, the measured half life is twice as large as the experimental limit at this energy. (The same conclusion might have been drawn from fig. 11 by noting that its left-hand side has a slope corresponding to a half life of 7×10^{-11} sec.) We therefore give the value $T_{\frac{1}{2}} = (1.50 \pm 0.10) \times 10^{-10}$ sec for the 241 keV excited state of Em^{220}.

J. G. SIEKMAN[8] has measured this half life by the delayed coincidence method (centroid shift), using a resolving time of about 7×10^{-9} sec. He measured coincidences between alpha particles and the K conversion line of the 241 keV gamma ray focused in a magnetic spectrometer. His result, $T_{\frac{1}{2}} = (3.1 \pm 1.1) \times 10^{-10}$ sec, differs from the present result by a factor of 2, but his lower limit of error is not far above our value.

(e) Em^{222} (187 keV)

Ra^{226} (1620 *y*) is an alpha emitter having a 6 % branch to the 187 keV excited state of Em^{222} (3.8 *d*).* The further descendants are the well-known radium series ending at Pb^{206}. Ra^{226} free of its decay products was prepared in the following way. A few μg of $RaCl_2$ were dissolved in 0.1 N HCl and absorbed on a cation exchange column, which was then eluted with 7 N HCl. The drops coming out of the column were collected on separate counting discs and dried. These samples were counted in an alpha counter, and their decay was followed for 24 hours; in addition, their gamma activity was checked, using a sodium iodide scintillator and an oscilloscope displaying the pulse height spectrum. The radium fraction was clearly identified at the expected elution position; lead, bismuth, and (presumably) polonium were eluted first, followed by radium. The radium was found to be quite pure. It was stored in a solution of 0.1 N HCl through which air was bubbled, so that Em^{222} and its short-lived daughters were prevented from growing in. The source was mounted just before the beginning of the lifetime measurements which were completed within 6 hours.

The Ra^{226} source material was mounted directly on a 10 mg/cm^2 plastic phosphor, and covered with enough aluminium (6.3 mg/cm^2) to prevent any alpha particles from reaching the electron counter. The latter, as usual,

* While this manuscript was in preparation, FOUCHER published a value for the half life of this excited state. His value, $(3.5 \pm 1.0) \times 10^{-10}$ sec, is in good agreement with ours (R. FOUCHER, Comptes Rend. **249**, 2310 (1959)).

was a 2 mm thick plastic phosphor. The pulse spectrum of the electron counter in coincidence with alpha particles showed a large peak corresponding to LMN . . . conversion of the 187 keV gamma ray. A pulse height window was set on this peak. The time analysis of the resulting alpha-electron coincidences is depicted in fig. 12. The curve shows a clean decay, giving a value $T_{\frac{1}{2}} = (3.2 \pm 0.2) \times 10^{-10}$ sec for the 187 keV excited state of Em^{222}.

(f) Ra^{226} (68 keV)

The half life of the 68 keV excited state of Ra^{226} has been measured by VARTAPÉTIAN and FOUCHER[9] using the delayed coincidence method (centroid shift), with resolving time 8×10^{-9} sec. They found $T_{\frac{1}{2}} = (6.3 \pm 0.7) \times 10^{-10}$ sec.

The 68 keV level of Ra^{226} is excited by a 24 % branch in the alpha decay of Th^{230} (ionium, 8×10^4 *y*). This activity was obtained from a one year old source of Th^{234} (24 *d*), containing some Th^{230}. The source was originally made by extracting thorium from reactor grade natural uranyl nitrate, and very carefully purifying the thorium fraction. In natural uranium, U^{238} and U^{234} are in radioactive equilibrium. U^{238} gives rise to the Th^{234} activity, while U^{234} decays into Th^{230}. In view of the very long half life of Th^{230}, only a very small amount of activity will have grown in. From the alpha activity present in the source we concluded that the Th^{230} had grown in for about two years, which appears reasonable. The alpha activity was 0.03 μC. In order to check the purity, an alpha spectrum was made, using a Frisch grid ionization chamber.* The spectrum showed only one group of alpha particles with energy 4.66 Mev, as expected (actually 4.68 and 4.61 Mev, unresolved). The beta activity (Th^{234}) was about 0.01 μC, but this contamination could not interfere with the measurements.

The procedure for measuring this half life was exactly the same as for the 84 keV level of Ra^{224}, described in (*c*) above. The time analysis for the present case is shown in fig. 13. This particular source was ideal in strength and thinness, and it yielded the best decay curve observed in this study. (Few radioactivities of whatever lifetime have had their decay plotted over five decades in a single experiment.) The half life found from this curve is $(6.3 \pm 0.2) \times 10^{-10}$ sec, the assigned error of 3 % being entirely due to uncertainty of the time-to-amplitude calibration. It is gratifying that the previous measurement of VARTAPÉTIAN and FOUCHER agrees exactly with this value.

* We are indebted to Mag. N. O. ROY POULSEN for making this measurement.

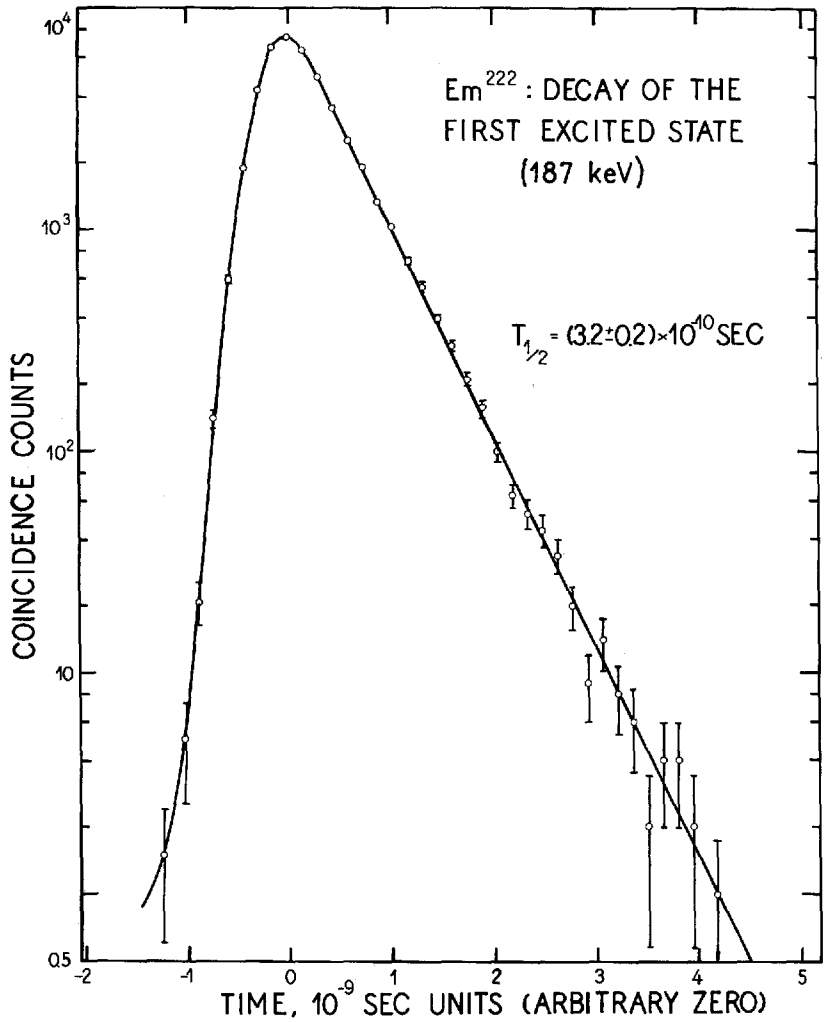

Fig. 12. The time analysis of the decay of the first excited state of Em^{222}.

(g) Th^{234} (48 keV)

The 48 keV excited state of Th^{234} is excited by a 23 % branch in the alpha decay of U^{238}. The difficulty in using this source is that pure U^{238} metal has a specific activity of only 12 disintegrations per second per milligram, and yet the source to be used must be thin both for $\approx$ 44 keV MN...

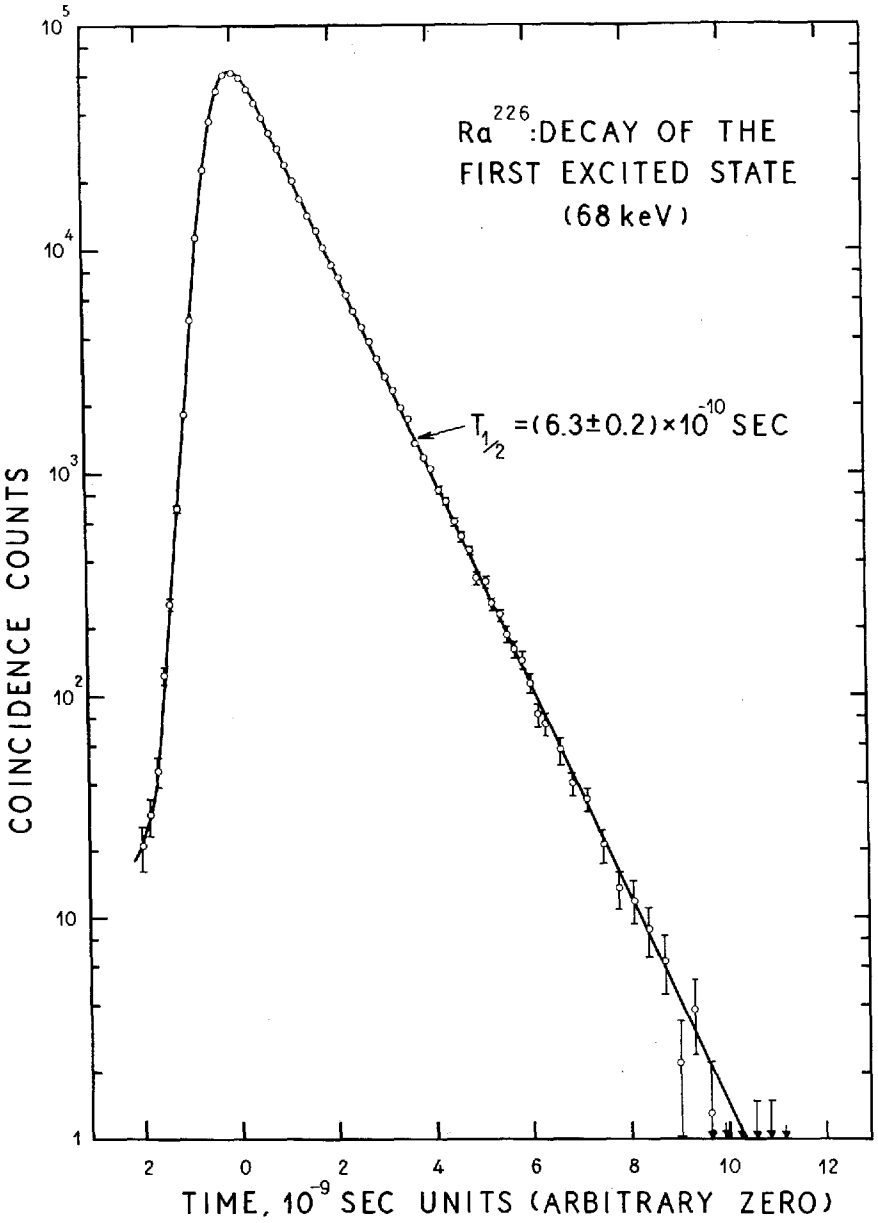

Fig. 13. The time analysis of the decay of the first excited state of Ra^{226}.

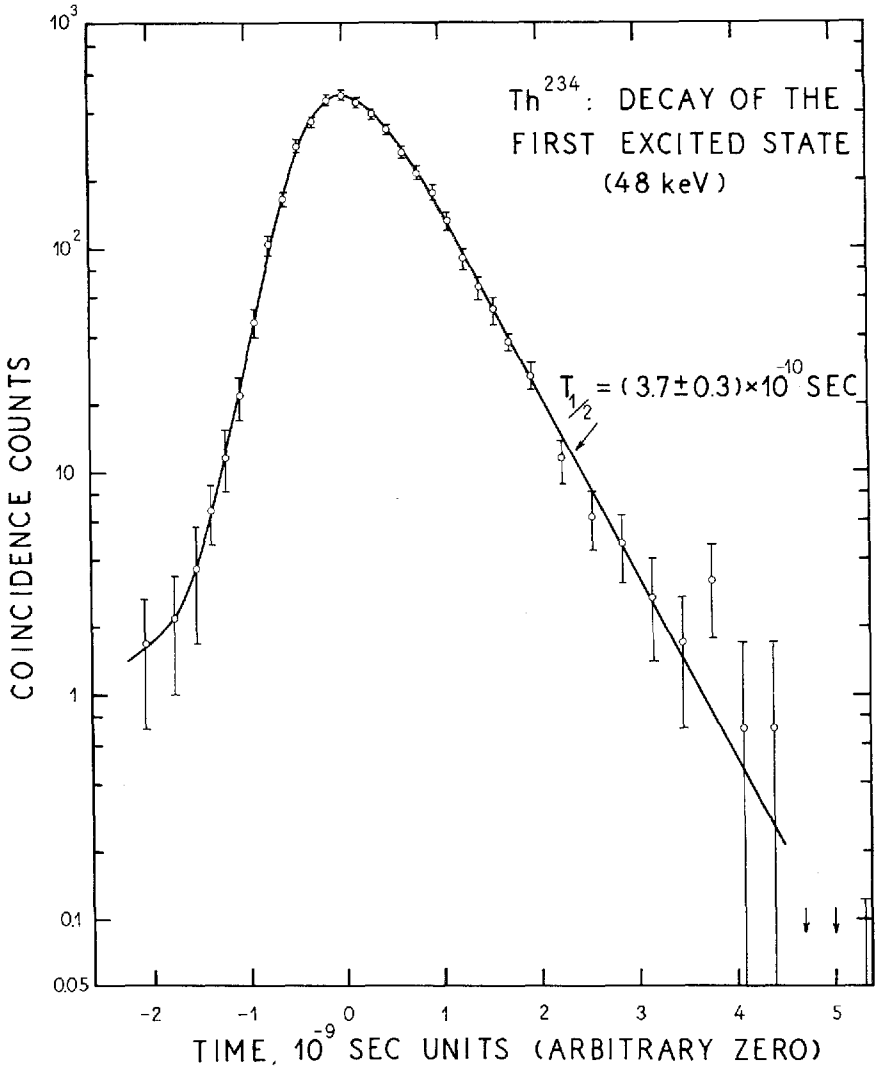

Fig. 14. The time analysis of the decay of the first excited state of Th^{234}.

conversion electrons and for 4 MeV alpha particles. A further difficulty lies in the presence of U^{234} (2.5×10^5 *y*), which exists in ordinary uranium in radioactive equilibrium with U^{238}. U^{234} decays to Th^{230}, populating the 53 keV excited state of Th^{230} with an intensity of 28 %. A measurement on ordinary uranium chemically freed of its decay products (except, of course,

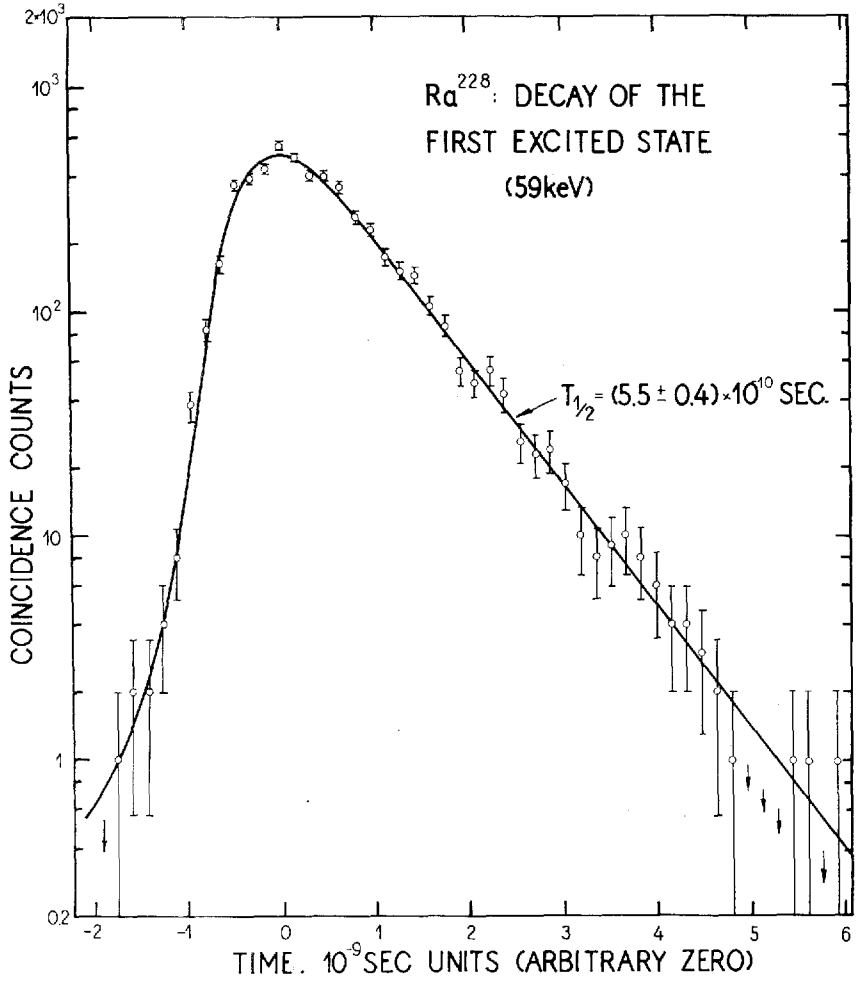

Fig. 15. The time analysis of the decay of the first excited state of Ra^{228}.

U^{234}) would give a mixture of the half lives of the Th^{234} and Th^{230} excited states.

The low specific activity must be accepted, implying very low counting rates in the experiment; the U^{234} admixture difficulty was avoided by using a supply of uranium depleted in U^{235} and hence *a fortiori* in U^{234}. The depletion figure for U^{234} was not known for this uranium sample. It was determined by preparing duplicate sources of normal and depleted uranium, as described below, and measuring their alpha activity with a 2π propor-

tional flow counter. A source of U^{238} alone, freed from all other radioactive products, should show a specific activity almost exactly half that of a source of normal uranium, the contribution from U^{235} being only 2.5 %. The counting results showed that the abundance of U^{234} in our depleted sample was approximately $^1/_7$ of the equilibrium amount. This amount would still be sufficient to require a correction in the measured result for the half life of the Th^{234} excited state, if it were not for the fact that the half life of the Th^{230} excited state, already measured, turns out to be exactly the same. We can therefore take the measured value for Th^{234} without further correction. Before mounting the source, the uranium was freed of its decay products, Th^{234} (24 *d*) and Pa^{234} (1.1 *m*). The starting material, UO_2, was dissolved in concentrated nitric acid, and oxidised to the uranium (VI) state. The solution thus contained $UO_2(NO_3)_2$ which can be extracted into ether, leaving all thorium in the aqueous phase. From the ether phase a very small volume, corresponding to the desired amount of uranium, was taken out and added to about 200 μl of a 0.01 % solution of insulin in water.

This purified $UO_2(NO_3)_2$ solution was deposited on the surface of a 0.15 mg/cm^2 aluminium foil, which in turn was on the surface of a 10 mg/cm^2 plastic phosphor disc, 2 cm in diameter. The solution was spread as uniformly as possible over this area of ≈ 3 cm^2, and evaporated to dryness, the insulin acting as a wetting agent and improving the evenness of the deposit. The total alpha activity of the source was about 6 disintegrations per second, implying a total mass of U^{238} of about 0.5 mg, and an average thickness about 0.2 mg/cm^2. Non-uniformity of the deposit probably raised the effective thickness somewhat above this amount. The source was covered with a second 0.15 mg/cm^2 aluminium foil, and a 3 mm thick plastic phosphor disc to serve as electron counter. The apparently wasteful use of the layer of aluminium foil on both sides of the source was judged to be necessary in order to prevent absorption of scintillation light by the yellow $UO_2(NO_3)_2$ deposit.

The source produced a recognizable peak in the alpha singles spectrum (with, of course, very bad statistical errors), and an alpha-coincident electron spectrum extending to the correct maximum pulse height, but having no recognizable peak owing to source thickness effects. These results agreed with expectation. The total coincidence counting rate between the chosen alpha pulses and the chosen electron pulses was about one count per minute. The time analysis recorded in a 70-hour run is shown in fig. 14. The half life of the Th^{234} excited state read from this curve is $(3.7 \pm 0.3) \times 10^{-10}$ sec; on account of the relatively large statistical errors, the assigned error is

somewhat larger than usual. (In assessing the drawing of the curve through the measured points, the reader should note that the last three plotted points on the right, all lying above the drawn curve, are balanced by two points, indicated by small arrows, which lie below the curve.)

(h) Ra^{228} (59 keV)

The 59 keV excited state of Ra^{228} is excited by a 24 % branch in the alpha decay of Th^{232}. All the remarks just made about using U^{238} as a source apply to an even greater extent to Th^{232}, whose specific activity is only 4 disintegrations per second per milligram. In addition, sources of thorium depleted in Th^{228} (1.9 *y* radiothorium) are not readily available. There is one factor in favour of the thorium case, compared with uranium; the conversion electrons of the 59 keV transition are higher in energy than the corresponding ones from a U^{238} source, because of the higher transition energy and lower atomic binding energies. Thus we may hope to use the *L* conversion electrons ($\approx$ 42 keV) as well as the MN. . . conversion electrons ($\approx$ 56 keV), gaining a factor of 4 in intensity.

The source used in the measurements was prepared in the Copenhagen isotope separator[10], through the kind cooperation of Ing. O. Skilbreid. The charge material for the ion source of the separator was 2 g of ThO_2 that had been chemically freed of its decay products (except, of course, Th^{228}). The ion source was run with a mixture of CCl_4 vapour and Cl_2 as the working gas, and produced a strong beam (50 to 100 μA) of $(Th^{232})^+$ ions. Since the nearest mass was four units away from Th^{232}, the separation was exceptionally clean. The ion beam struck a graphite plate placed 15 mm above the source holder, and metallic Th^{232} sputtered from the graphite surface onto the source holder. This procedure involves a loss of a factor of 5 in separated material, but it makes it easier to get a uniform deposit over a large area, and it avoids the necessity of dissipating the ion beam power ($\approx$ 3 watts) in the source holder. Experience with the Van de Graaff targets prepared in this way has shown that the number of carbon atoms carried onto the target is negligible for our purposes. The separation proceeded for about 30 hours, the source holder being rotated periodically during this time to ensure uniformity. The source holder, as in the uranium case just discussed, was a 2 cm diameter disc of 10 mg/cm^2 plastic phosphor, covered with a 0.15 mg/cm^2 aluminium foil. The total activity of the source at the end of separation was about 2.4 disintegrations per second, implying a

total mass of 0.6 mg, or an average density of 0.2 mg/cm². Both visual inspection and rough alpha counting showed that the deposit was very uniform. Its appearance was that of a slightly tarnished bright metal.

The Th^{232} source was mounted as in the U^{238} case just discussed, and counter settings much the same were used. The advantages of electron energy and source uniformity outweighed the disadvantage in specific activity, however, and the coincidence counting rate was about three times better than for the uranium source, viz., 3 counts per minute. The time analysis was run for 45 hours, and the result is shown in fig. 15. The half life of the 59 keV excited state of Ra^{228} is found to be $(5.5 \pm 0.4) \times 10^{-10}$ sec.

(i) Th^{228} (57.8 keV)

The 57.8 keV first excited state of Th^{228} is strongly excited in the beta decay of Ac^{228} (6.1 *h*). Two beta branches of maximum energy 2.1 and 1.8 MeV, totalling 25 % of the disintegrations, feed almost directly into the desired state. Further beta branches, of energy 1.1 MeV or less, feed higher excited states which then emit a variety of gamma rays. The half life of the 57.8 keV state was measured by analyzing coincidences between the high energy beta branches and the MN... conversion electrons of the 57.8 keV state, thus avoiding most of the prompt coincidences that would otherwise occur.

The Ac^{228} activity was obtained from a sample of Ra^{228} (MsTh 6.7 *y*), which was in partial equilibrium with its daughters. These are the same as the ones dealt with under Ra^{224}, section (*c*), plus of course Ac^{228}. Again a cation exchange procedure was used to prepare the source. The mixture of isotopes was absorbed from a very dilute hydrochloric acid solution (0.01 N) onto a cation exchange column which had previously been conditioned with a 0.05 M solution of $(NH_4)_2$EDTA (ethylene-diamino-tetraaceticacid-diammonium salt) (pH 4.7) and then washed with water. All activities were absorbed in a band on the top of the resin filling. The column was first eluted with 0.005 M $(NH_4)_2$ EDTA (pH 4.7) which removed thorium, lead, and bismuth, leaving radium and actinium behind. The concentration of the eluant was then increased to 0.05 M. This took out Ac^{228}. The fraction used had a purity of about 95 % by beta activity, the impurities being Pb^{212} and Bi^{212}.

The Ac^{228} activity was deposited directly on the surface of a plastic phosphor 3 mm thick, and had a surface density of about 100 μg/cm² (con-

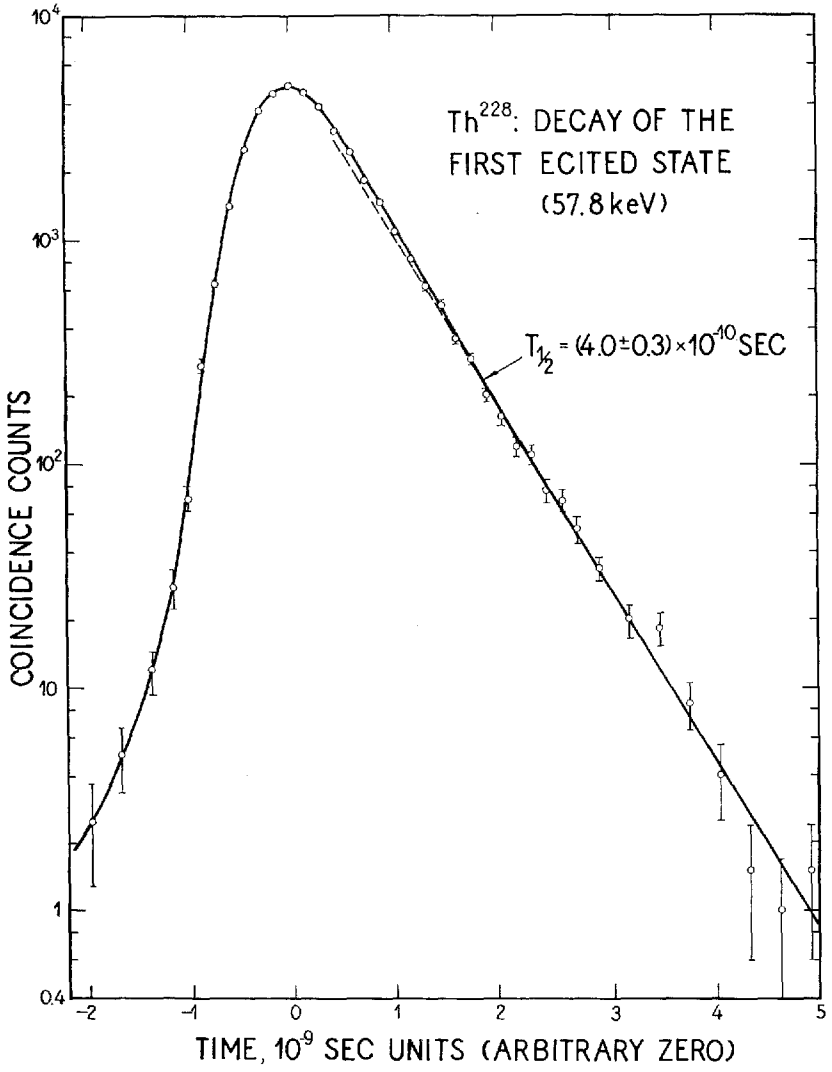

Fig. 16. The time analysis of the decay of the first excited state of Th^{228}. Note that a few prompt coincidences occur in this curve (see the text, section (i)).

sisting mainly of the organic eluant material). This phosphor detected the conversion electrons; it was covered with 30 mg/cm² of aluminium and then with a second 3 mm thick phosphor to serve as beta counter. Pulses from this counter lying between 1.0 and 1.6 MeV were accepted as the beta events. The spectrum of the conversion electron counter in coincidence with these

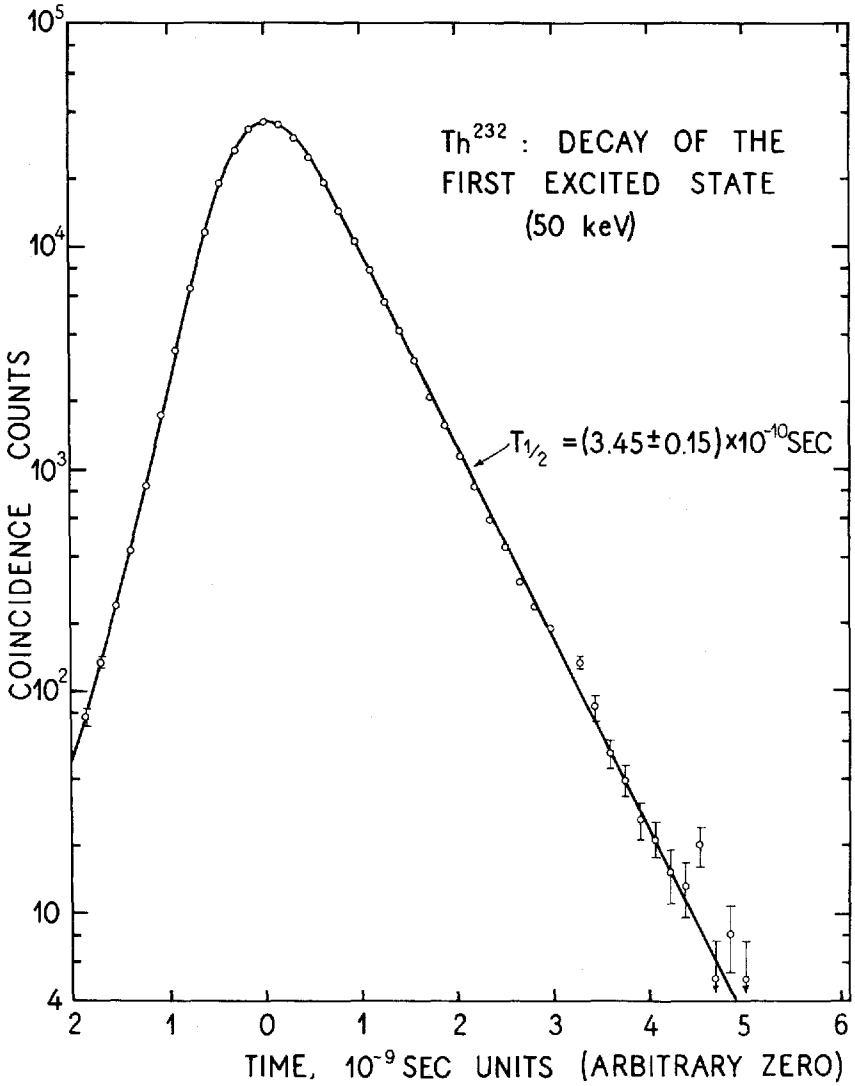

Fig. 17. The time analysis of the decay of the first excited state of Th^{232}.

pulses showed a peak from L conversion of the 57.8 keV transition, with a bump on its upper energy edge due to MN... conversion electrons. In addition, there was a low background due to coincidences between nuclear beta rays detected in the conversion electron counter and high energy gamma rays detected in the beta counter. These coincidences would give rise to prompt events in the time analysis amounting to about 15 % of the

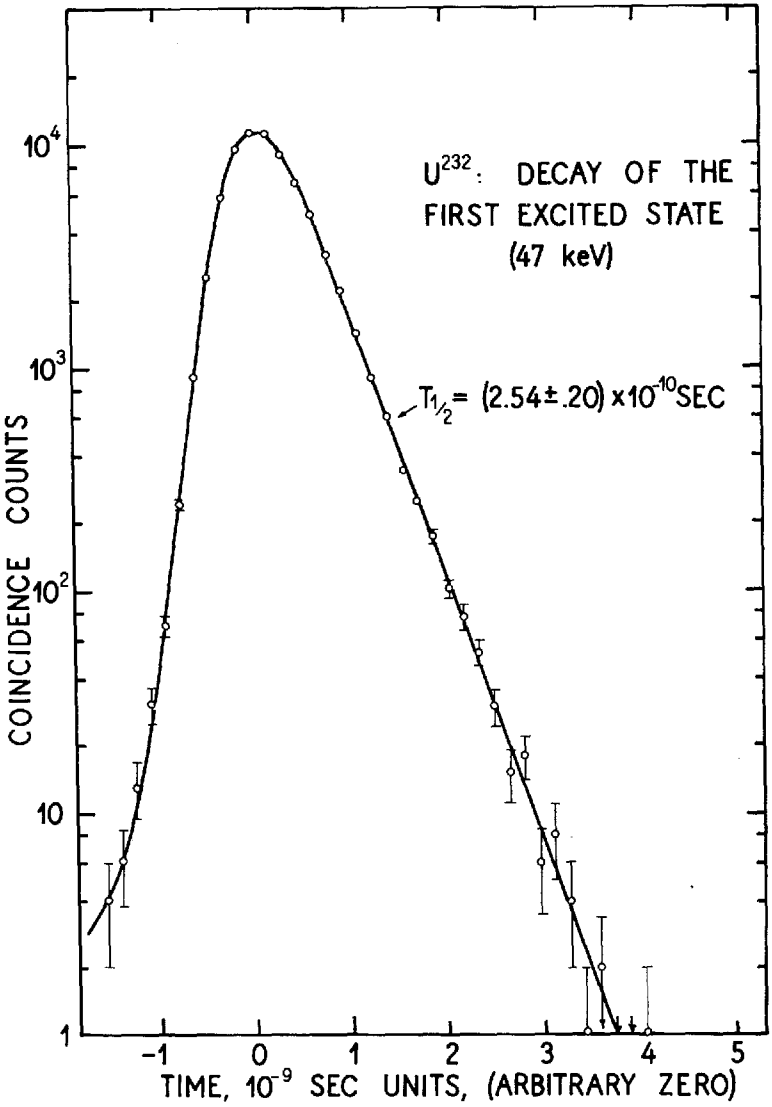

Fig. 18. The time analysis of the decay of the first excited state of U^{232}.

total. The time analysis, fig. 16, shows the expected small prompt component, together with a clean decay of half life 4.0×10^{-10} sec. If the presence of the prompt coincidences had been ignored and a straight line drawn through the points, the half life would have appeared about 5 % lower. We assign a slightly larger than usual error, and give for the 57.8 keV excited state of Th^{228} the value $T_{\frac{1}{2}} = (4.0 \pm 0.3) \times 10^{-10}$ sec.

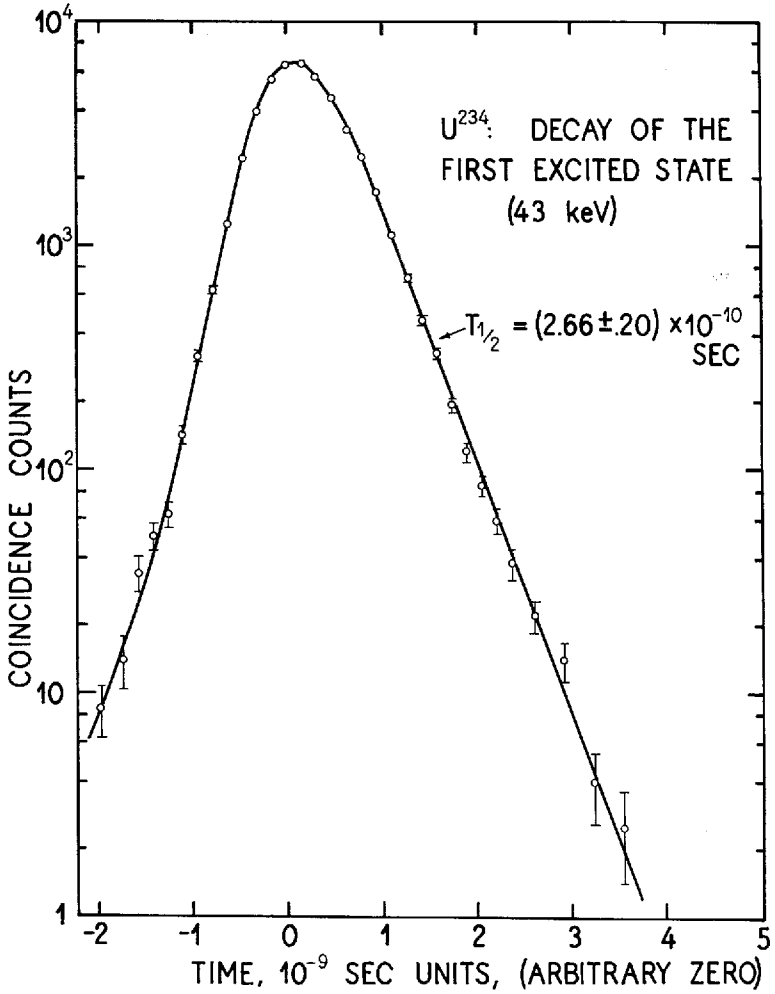

Fig. 19. The time analysis of the decay of the first excited state of U^{234}.

(j) Th^{232} (50 keV), U^{232} (44 keV), U^{234} (43 keV) U^{236} (45 keV), Pu^{238} (44 keV), and Pu^{240} (43 keV)

These six excited states were studied in radioactive sources supplied through the kind cooperation of Dr. E. P. STEINBERG of the Argonne National Laboratory. The parent source in each case is an alpha emitter with about 25 per cent branching to the first excited state of the daughter. (The parents

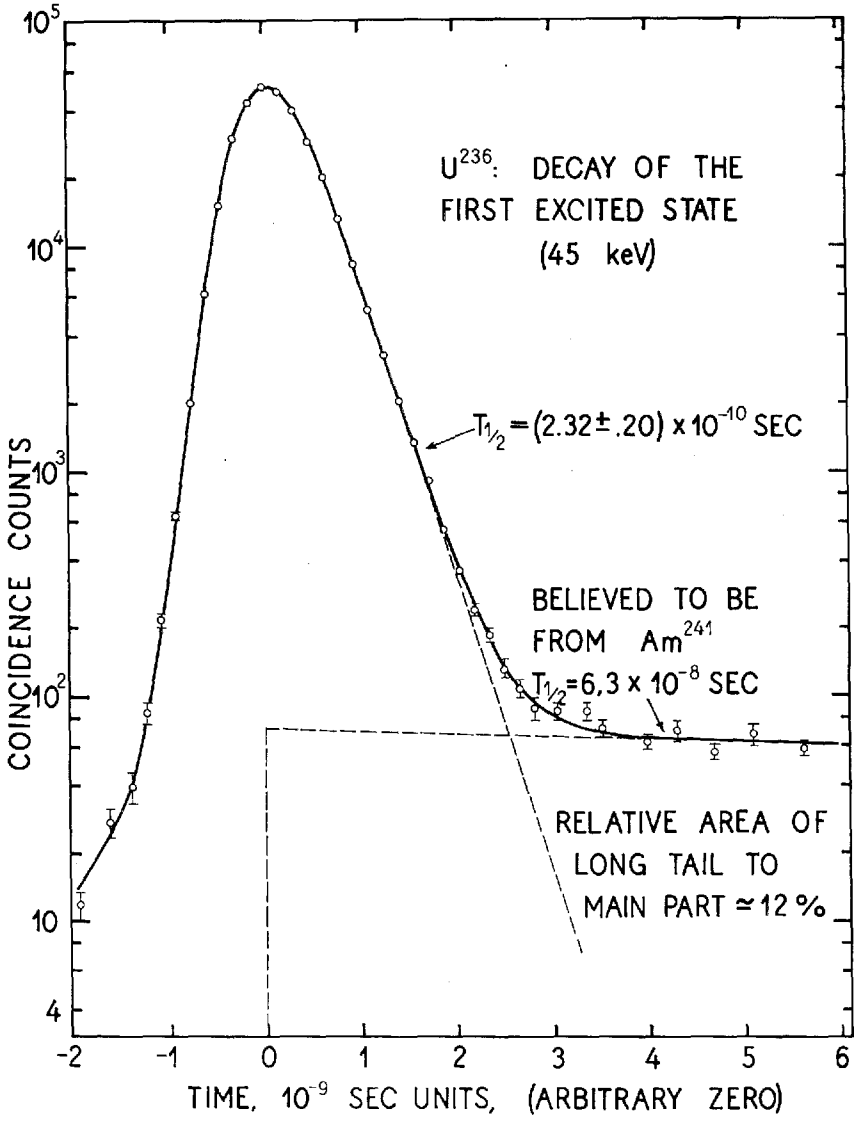

Fig. 20. The time analysis of the decay of the first excited state of U^{236}. A long lived contribution has been subtracted (believed to be from Am^{241}).

are, in order, U^{236}, Pu^{236}, Pu^{238}, Pu^{240}, Cm^{242}, and Cm^{244}). Each source was supplied already deposited on the surface of a 10 mg/cm² plastic phosphor, with an average strength of a thousand disintegrations per second. On

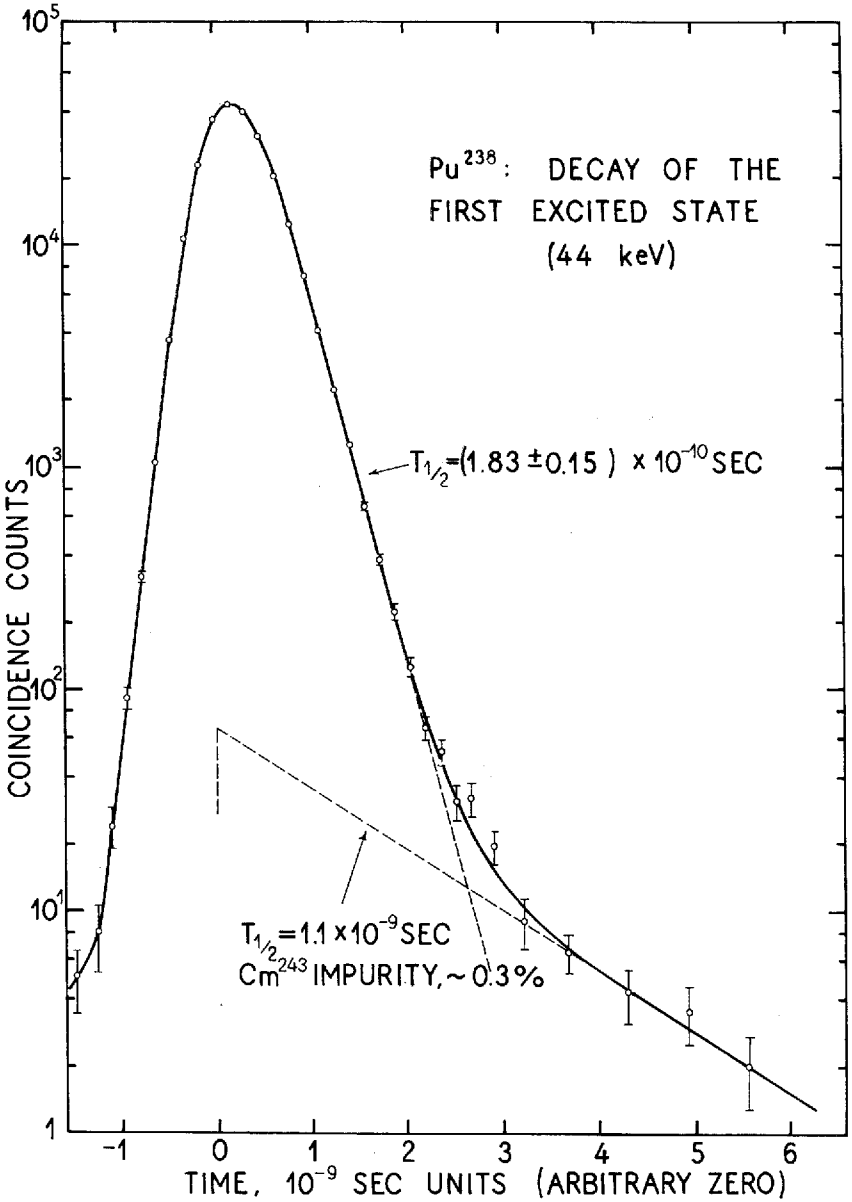

Fig. 21. The time analysis of the decay of the first excited state of Pu^{238}. A long lived impurity has been subtracted (believed to be from Cm^{243}).

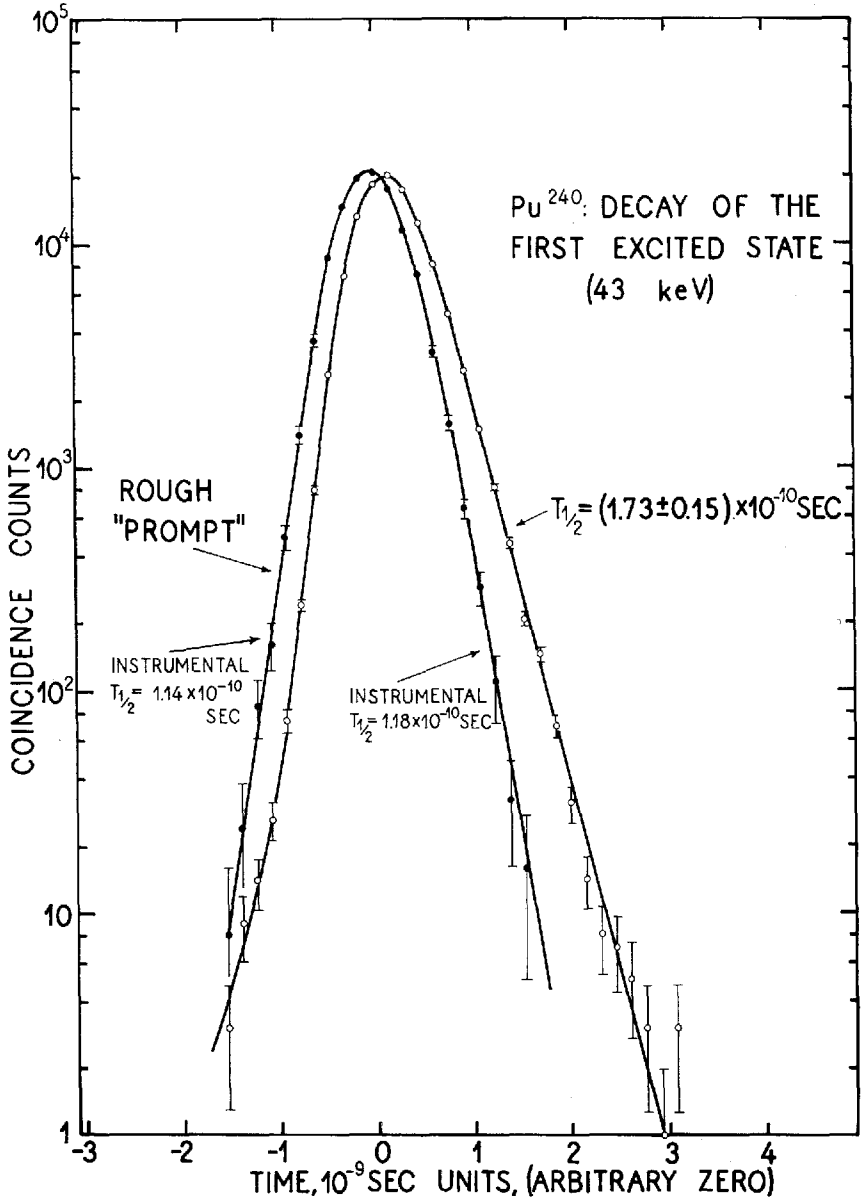

Fig. 22. The time analysis of the decay of the first excited state of Pu^{240}. A prompt curve is included for reference.

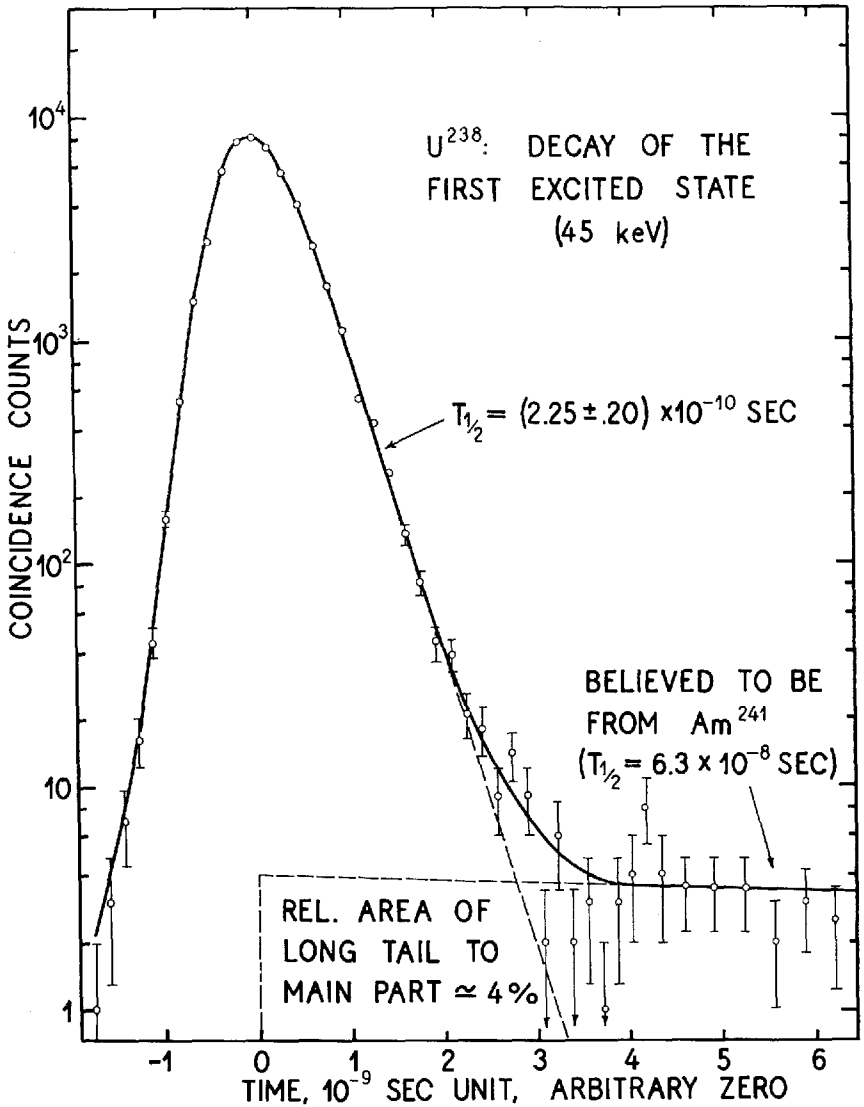

Fig. 23. The time analysis of the decay of the first excited state of U^{238}. A long lived contribution has been subtracted (believed to be from Am^{241}).

account of the small penetrating power of the LMN... conversion electrons, the thin phosphor on which the source was deposited was used in each case as the electron counter. The source deposit was covered with a

layer of 0.15 mg/cm^2 aluminium foil, and a second thin plastic phosphor was pressed against the foil to serve as an alpha counter. The conversion electron counter bias was set to accept energies from 30 to 50 keV, approximately. In this way the MN... conversion lines, and perhaps the upper edge of the L conversion line, were detected. The alpha pulse height window covered the broad alpha peak in the usual way. No trouble was experienced with any of the sources, and the six measurements were completed in as many days.

The result for the 50 keV first excited state of Th^{232} is shown in fig. 17. The half life is $(3.45 \pm 0.15) \times 10^{-10}$ sec. This nuclide is one of two for which the corresponding Coulomb excitation measurement has been made by SKURNIK *et al.*[11], the other being U^{238}.

The curves for U^{232} (47 keV) and U^{234} (43 keV) appear in figs. 18 and 19, with half lives $(2.54 \pm 0.20) \times 10^{-10}$ sec and $(2.66 \pm 0.20) \times 10^{-10}$ sec, respectively.

Fig. 20 shows the curve for U^{236} (45 keV), measured from a parent source of Pu^{240}. The weak component of longer lifetime is tentatively identified as due to the presence of Am^{241} impurity in the source. Am^{241} (458 y) has an 85 % alpha branch to an excited state at 60 keV whose half life is known to be 6.3×10^{-8} sec, consistent with our measured curve. It is a logical impurity in a Pu^{240} source, because it can be formed by the beta decay of Pu^{241} (13 y). The long lived component is subtracted in fig. 20, giving a half life for the 45 keV first excited state of U^{236} of $(2.32 \pm 0.20) \times 10^{-10}$ sec. It is clear that exact knowledge of the half life of the subtracted component in fig. 20 is not required in any case.

Fig. 21 shows the curve for Pu^{238} (44 keV), measured from a parent source of Cm^{242}. Again we have a longer lifetime due to an impurity, in this case Cm^{243}, which decays to an excited state of Pu^{239} having a half life of 1.1×10^{-9} sec. Making the subtraction, we arrive at a half life of $(1.83 \pm 0.15) \times 10^{-10}$ sec for the 44 keV state of Pu^{238}.

Fig. 22 shows the curve for Pu^{240} (43 keV), with a comparison curve labelled "rough prompt". This prompt curve was made by the same technique of light leakage as that described in section (a) above. It was included at this point in the measurements because the Pu^{240} excited state has the shortest half life of any of the transitions below 100 keV. The instrumental half lives read from the slopes of the two sides of the prompt curve lie between 1.1 and 1.2×10^{-10} sec, while the half life of the 44 keV excited state of Pu^{240} is $(1.73 \pm 0.15) \times 10^{-10}$ sec. Fig. 22 thus shows that we are still far enough from the instrumental limit to make a slope measurement of this

half life at this energy, but it also suggests that the still shorter half lives anticipated for the first excited states of curium and californium would be much more difficult to measure.

(k) U^{238} (45 keV)

The 45 keV first excited state of U^{238} is excited by a 24 % branch in the alpha decay of Pu^{242} (3.8×10^5 *y*). The Pu^{242} sample was also provided by the Argonne National Laboratory through the kindness of Dr. STEINBERG.

The sample contained 97.3 % Pu^{242} by weight, but, owing to its long half life, the Pu^{242} activity only represented 6.4 % of the total alpha activity; the main activity was Pu^{238} (86 *y*). In this case, therefore, an isotope separation was essential. The alpha activity due to Pu^{242} in the sample was 3,200 disintegrations per second, corresponding to 20 μg of plutonium. The ion source of the isotope separator could not be expected to work on such a small mass. The sample was therefore mixed with 1 mg of uranium oxide, and a procedure similar to the one described in section (*h*) was used, except that the activity was collected directly on a 0.15 mg/cm^2 collector foil of aluminium. The result was a source of Pu^{242} 1 mm wide and 8 mm long, having 170 alpha disintegrations per second, corresponding to 5 % yield in the mass separation. The source was mounted in the usual way and counter settings similar to those of section (*j*) were employed. The delay curve is shown in fig. 23. It can be seen that there is a long-lived tail present in the distribution. This is believed to be due to small amounts of Am^{241} (458 *y*) present in the source as an impurity. The presence of some Am^{241} is reasonable, even in the mass-separated source, because its mass is adjacent to that of Pu^{242}. The 6.3×10^{-8} sec half life produced by Am^{241} has been discussed in section (*j*), under U^{236} (see also fig. 20). The alpha decay energy of Am^{241} (5.57 MeV) differs appreciably from that of Pu^{242} (4.94 MeV), and it was possible to discriminate against Am^{241} by using a narrow channel in the region of 5 MeV for the pulses from the alpha counter. The poor resolution of the plastic phosphor limits the effectiveness of this procedure, but the Am^{241} contribution was reduced to 4 % (see fig. 23) from a value of 12 % when a wide window was used. After the usual subtraction, fig. 23 gives $(2.25 \pm 0.20) \times 10^{-10}$ sec for the half life of the 45 keV excited state of U^{238}. The corresponding Coulomb excitation measurement has been made for this nuclide[11].

3. Discussion

Before evaluating the experimental results, we consider how well the rotational model applies to them. In fig. 24 we have plotted the energy of the first excited state, E_1, and the ratio of the energy of the second excited state to that of the first excited state, E_2/E_1, as functions of A for the nuclides of this study. For the rotational description to be valid, E_1 should be low and relatively independent of A. One suggested criterion[1] for what is meant by "low" is that E_1 should be below

$$E_1 \simeq 13\,\hbar^2/\Im_{\text{rig}}. \tag{8}$$

This critical value of E_1 is calculated to be 109 keV for Ra^{222}, the left hand radium point in fig. 24; the experimental value of E_1 for the same nucleus is 111 keV. We may thus accept all the nuclides except the emanation isotopes as "rotational", on this criterion. Fig. 24 also shows that the values of E_2/E_1 for all the nuclides except the emanation isotopes are near the rotational value 3.33, as deduced from equation (1). For the emanation isotopes, the values of E_2/E_1 lie closer to the value 2.0, characteristic of vibrational excitations. (In any case their second excited states are of 2+ character, rather than the 4+ required in a rotational model.) Both of our criteria therefore suggest that the rotational description is not a good one for emanation isotopes, i.e., that the emanation isotopes are nearly spherical. We will nevertheless evaluate the emanation results in the same way as the others, enclosing the resulting values in brackets in tables and graphs as a warning. (The values of $B(E2;\,0 \to 2)$ are correct, independent of assumptions about nuclear shape.)

We note that in this region the question of whether a nucleus is spherical or deformed is decided primarily by the proton number Z, the change from spherical to deformed occurring between $Z = 86$ (emanation) and $Z = 88$ (radium). In the rare earth region, the change occurs between neutron numbers $N = 88$ and $N = 90$. The calculated particle energy levels in a deformed potential of NILSSON[12] are consistent with these facts.

The first step in treating the experimental half lives is to calculate the values of $B(E2;\,0 \to 2)$ in units of $e^2 \times 10^{-48}\,\text{cm}^4$ by means of

$$B(E2;\,0 \to 2) = 282\,[T_{\frac{1}{2}}\,(1+\alpha)\,E_\gamma^5]^{-1}, \tag{9}$$

which follows from (2) and (3), with E_γ in keV. The values of E_γ are those quoted in the preceding experimental sections. The values of α were ob-

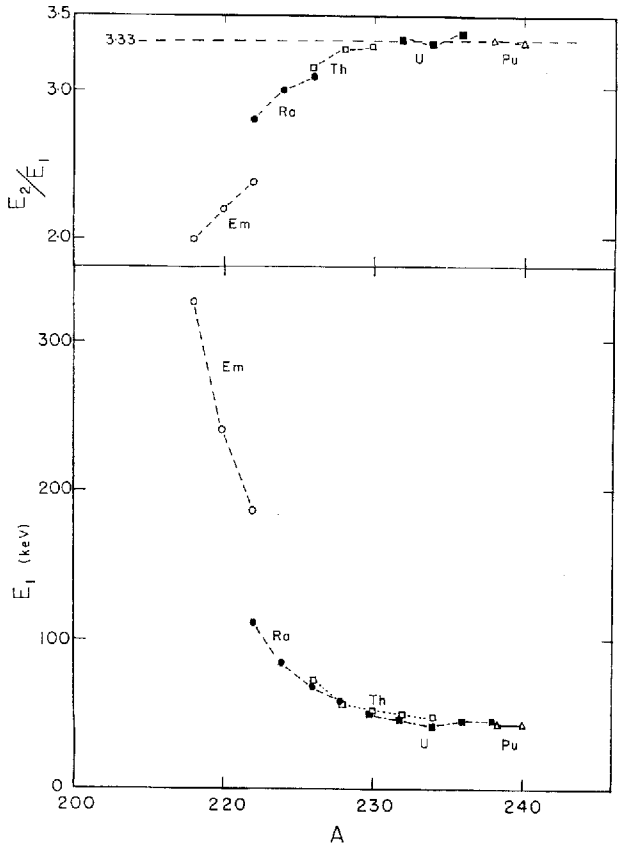

Fig. 24. (Lower part). The energy E_1, of the first excited states of each of the even nuclei used in this experiment, plotted as a function of A. The energies for the three Em isotopes are too high for a rotational description to apply (see the text).
(Upper part). The ratio, E_2/E_1 of the energies of the second and first excited states. The ratios for the three Em isotopes lie closer to the value 2.0 (vibrational excitations) than to 3.33 (rotational excitations). In addition, the second excited states in the Em isotopes are 2+, rather than 4+ as required on the rotational model.

tained by interpolation in the K and L conversion tables of Rose[13], with the additional assumption, based on experiment, that MN... conversion is always one-third of L conversion. No additional error has been assigned for this procedure, because the results could be corrected if better conversion tables should become available. The energy values, E_γ, often have uncertainties of two per cent or so, and at first glance this error would appear to be serious, owing to the high power of E_γ in (9). In fact, however, α is large compared with unity, and varies approximately as E_γ^{-5}. The factor

$(1+\alpha)\,E_\gamma^5$ appearing in (9) is therefore almost independent of energy, and moderate errors in the values of E_γ contribute negligible errors to the final results. The same effect accounts for the fact, at first sight remarkable, that all the experimental half lives lie in the narrow range 1.5×10^{-10} to 7.6×10^{-10} sec. Moreover, most of this variation is due to actual variations in $B(E2)$ and to the variation of α with Z, rather than to variations in E_γ.

Table I lists the nuclides measured (col. 1), the values of E_γ (col. 2), the measured half lives (col. 3), the values of $(1+\alpha)$ used in applying (9) (col. 4), and the resulting values of $B(E2;\ 0\rightarrow2)$ (col. 5). Column 6 gives the results for $B(E2;\ 0\rightarrow2)$ for Th^{232} and U^{238}, measured by Coulomb excitation by SKURNIK *et al.*[11]. The discrepancies between their values and ours are 13 %, quite consistent with the combined errors of measurement. These two Coulomb excitation measurements were made by observing inelastically scattered protons or deuterons from the target, and are independent of internal conversion coefficients. The agreement between the two pairs of values may be interpreted as an indirect verification, within 15 %, of the computed $E2$ conversion coefficients of ROSE[13] for this region of Z and energy. The conversion coefficients involved are large (cf. col. 4 of table I), and it is unlikely that direct measurements of them will furnish any closer check of ROSE's values.

Column 7 of table I gives the values of Q_0 in units of 10^{-24} cm^2, derived from the $B(E2;\ 0\rightarrow2)$ values by means of

$$|Q_0| = [10.05\,B(E2;\ 0\rightarrow2)]^{1/2}, \tag{10}$$

which follows from (4). The errors shown for Q_0 and for $B(E2;\ 0\rightarrow2)$ in the table reflect only the errors assigned to the experimental half lives. Column 8 gives the values of β calculated from Q_0 by means of (5). At this point it is necessary to choose a value for R_0, the average nuclear radius. We have used $R_0 = 1.2\,A^{1/3}\times10^{-13}$ cm, so as to agree with other workers in this field, particularly MOTTELSON and NILSSON.[12] In that case, (5) becomes

$$\beta = 3.12\left[\left(1+\frac{59\,Q_0}{ZA^{2/3}}\right)^{1/2}-1\right]. \tag{11}$$

The fractional errors in β are closely the same as those in Q_0, ranging from 1.7 % to 5.5 %. Finally, column 9 gives the value of $\mathfrak{I}/\mathfrak{I}_{rig}$, with $\mathfrak{I}$ calculated from the observed energy of the first excited state by means of (1), and $\mathfrak{I}_{rig}$ calculated from (6), using the experimental values of β and the

TABLE I.

(1) Nuclide	(2) E_γ (keV)	(3) $T_{\frac{1}{2}}$ (10^{-10} sec)	(4) $1+\alpha$	(5) $B(E2;\ 0\rightarrow 2)$ ($e^2\ 10^{-48}$ cm^4)	(6) $B(E2;0\rightarrow 2)$ from Coulomb excitation	(7) Q_0 (10^{-24} cm^2)	(8) β	(9) $\Im/\Im_{\mathrm{rig}}$
Em^{218}	325	$\langle 0.8$	1.112	$\rangle$ 0.875	..	($\rangle$ 2.97)	($\rangle$ .085)	($\langle$ .081)
Em^{220}	241	1.50 ± 0.1	1.283	1.8 ± 0.12	..	(4.26 ± 0.14)	(0.121)	(0.106)
Em^{222}	187	3.2 ± 0.2	1.70	2.27 ± 0.14	..	(4.79 ± 0.15)	(0.136)	(0.135)
Ra^{222}	111	5.2 ± 0.4	7.36	4.37 ± 0.34	..	6.63 ± 0.26	0.184	0.223
Ra^{224}	84.4	7.6 ± 0.3	22.6	3.84 ± 0.15	..	6.21 ± 0.13	0.171	0.291
Ra^{226}	68	6.3 ± 0.2	59.6	5.17 ± 0.17	..	7.22 ± 0.12	0.197	0.351
Ra^{228}	59	5.5 ± 0.4	119.1	6.03 ± 0.44	..	7.79 ± 0.28	0.212	0.400
Th^{226}	72	3.95 ± 0.2	54.7	6.77 ± 0.34	..	8.25 ± 0.20	0.220	0.330
Th^{228}	57.8	4.0 ± 0.3	152	7.14 ± 0.54	..	8.47 ± 0.32	0.225	0.403
Th^{230}	53	3.7 ± 0.2	236	7.70 ± 0.63	..	8.80 ± 0.35	0.233	0.433
Th^{232}	50	3.45 ± 0.15	308	8.50 ± 0.37	9.7 ± 0.5	9.25 ± 0.23	0.243	0.450
Th^{234}	48	3.7 ± 0.3	377	7.98 ± 0.64	..	8.93 ± 0.35	0.233	0.467
U^{230}	51.7	2.6 ± 0.3	330	8.90 ± 1.00	..	9.46 ± 0.52	0.245	0.443
U^{232}	47	2.54 ± 0.2	490	9.90 ± 0.78	..	9.98 ± 0.28	0.257	0.470
U^{234}	43	2.66 ± 0.2	758	9.50 ± 0.72	..	9.77 ± 0.38	0.251	0.516
U^{236}	45	2.32 ± 0.2	614	10.70 ± 0.92	..	10.35 ± 0.44	0.263	0.485
U^{238}	45	2.25 ± 0.2	614	11.05 ± 0.98	12.6 ± 0.6	10.52 ± 0.48	0.268	0.480
Pu^{238}	44	1.83 ± 0.15	783	11.9 ± 1.0	..	10.95 ± 0.45	0.271	0.493
Pu^{240}	43	1.73 ± 0.15	880	12.6 ± 1.1	..	11.26 ± 0.48	0.278	0.488

This is a compilation of the experimental results from the previous section. The experimental energy of the first excited 2+ state is listed in column 2, the data coming from the nuclear tables of STROMINGER *et al.*[4] Column 3 lists the measured half lives and their absolute errors. Column 4 shows the quantity $(1+\alpha)$, where α is obtained from the tables of ROSE[13] by interpolation. The reduced transition probability, $B(E2)$, is shown in column 5. Column 6 gives the two available measurements from the Coulomb excitation data (by the kind permission of E. SKURNIK *et al.*[11]). The ground state quadrupole moments are listed in column 7. The deformation parameter β is given in column 8. The last column gives the ratio of the moment of inertia to that of a rigid rotor, $\Im/\Im_{\mathrm{rig}}$.

value of R_0 mentioned earlier. The simplified formula under these conditions is

$$\Im/\Im_{\mathrm{rig}} = 2.15 \times 10^5\,[E_\gamma A^{5/3}(1+0.31\beta)]^{-1}. \qquad (12)$$

The experimental uncertainty in β makes only a small contribution to the error in $\Im/\Im_{\mathrm{rig}}$, about comparable with the contribution from the uncertainty in E_γ. The values of $\Im/\Im_{\mathrm{rig}}$ thus have relative uncertainties of around two per cent.

Fig. 25 presents the results for $B(E2;\ 0\rightarrow 2)$ plotted as a function of A. An auxiliary ordinate scale on the right also shows the values of $|Q_0|$ for the

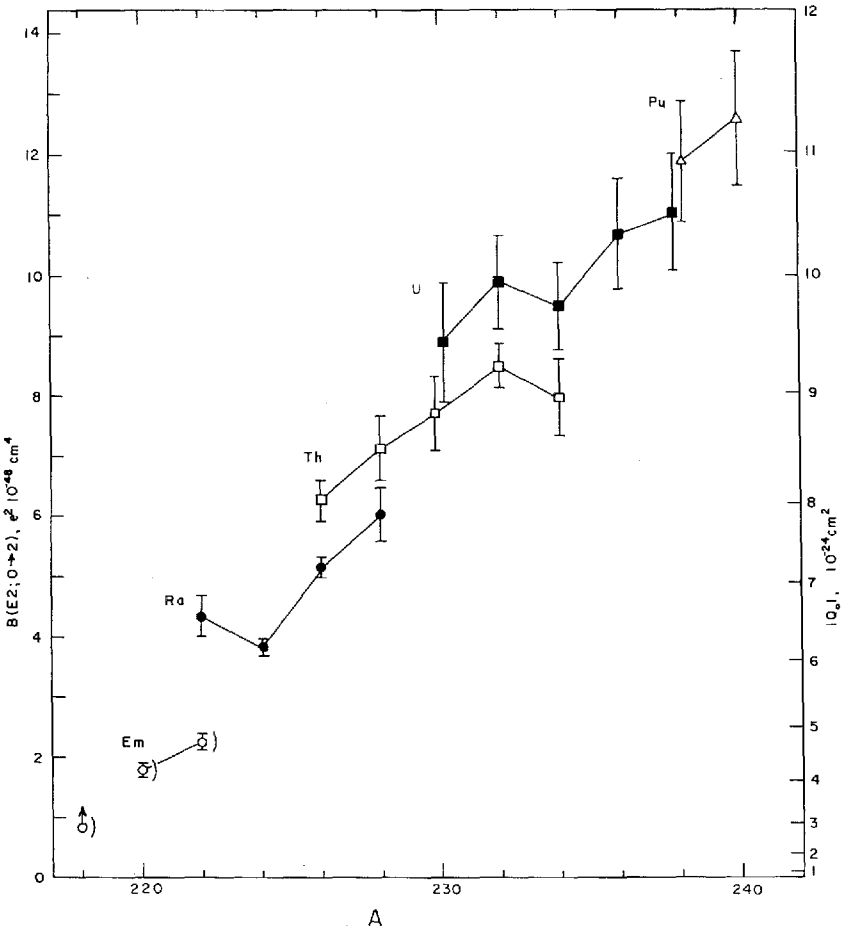

Fig. 25. The reduced transition probabilities, $B(E2;\ 0\rightarrow 2)$, plotted as a function of A. The right-hand ordinate refers to the corresponding intrinsic quadrupole moments, $|Q_0|$, calculated assuming the rotational model. The errors shown are the absolute ones, the relative ones being smaller by about a factor $^1/_2$. The half-brackets on the Em points show that the right hand $|Q_0|$ scale should not be taken seriously as far as they are concerned.

same plotted points. The error bars on the points represent the estimated absolute standard errors (but with no allowance for errors in α, as mentioned earlier). The relative errors can be taken as considerably smaller, perhaps by a factor 1/2. The plotted points have been joined in groups according to Z. It is clear that the $B(E2)$ or Q_0 values depend mainly on Z, with a residual tendency to increase with N. The detailed structure of the results, e.g., the low values at $A = 224$ and $A = 234$, is probably real, but we will not attempt any interpretation of these fine points.

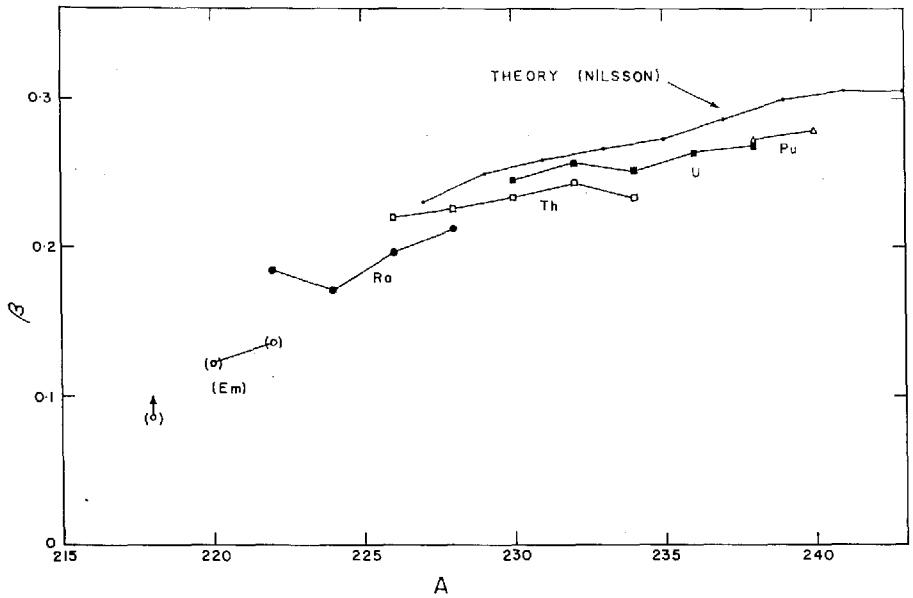

Fig. 26. The experimentally measured deformation parameters, β, assuming spheroidal nuclear shapes, plotted as a function of A. The theoretical curve is due to MOTTELSON and NILSSON[12]. The Em points have been placed in brackets as a warning (see the text).

Fig. 26 shows the experimental values of β plotted as a function of A, together with a theoretical line due to NILSSON (reference 12). The theoretical values represent the deformations which yield minimum nuclear energy for a model of independent-particle motion in a deformed potential. The actual values refer to particular odd mass nuclei in this region, and are therefore not expected to reproduce the experimental values in detail. In addition, the residual interactions are expected to reduce the deformations somewhat. Quantitative calculations of this effect have not yet been published.* With these remarks in mind, the agreement between theory and experiment is seen to be very good.

We turn now to the moments of inertia. Fig. 27 shows the experimental values of $\mathfrak{J}/\mathfrak{J}_{\text{rig}}$, plotted as a function of β. The diagram also includes a set of experimental values for the even rare earths, taken from ELBEK, OLESEN and SKILBREID[14]. The experimental values are indicated by circles. Crosses refer to preliminary theoretical values calculated by S. G. NILSSON and O. PRIOR.** Theoretical and experimental points belonging to the same

* Such calculations are at present in progress (Z. L. SZYMANSKI, private communication).

** We are indebted to Dr. S. G. NILSSON for making available the results of these calculations prior to publication.

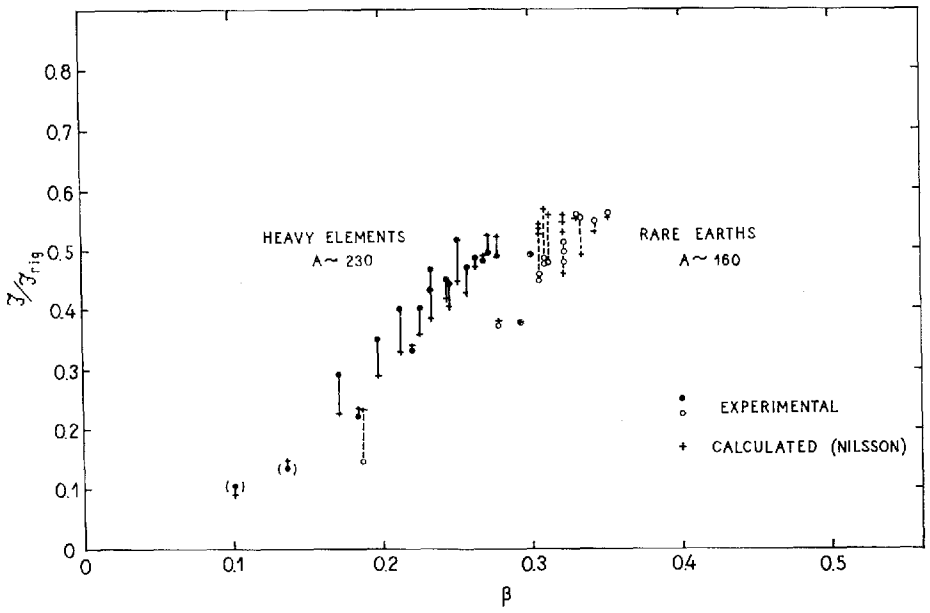

Fig. 27. The ratios of the moments of inertia to the rigid rotor moments of inertia, $\mathfrak{J}/\mathfrak{J}_{rig}$, plotted as a function of β. The results for even rare earth nuclei are taken from ELBEK, OLESEN and SKILBREID.[14] Two points for Em have been placed in brackets as a warning (see the text). Circles represent experimental points. Crosses are calculated values (see text).

nucleus are joined. The theoretical values have been calculated on the basis of individual-particle motion in a spheroidal field with pairing correlations added, using the general expressions derived by BELYAEV[15]. It is seen that the agreement between theory and experiment is quite satisfactory, especially in the heavy element region. The discrepancies found are on the average 10 %, while the experimental errors are of the order of 3 %.

We may summarize our conclusions by saying that recent theoretical calculations succeed very well in reproducing the general trends of the experimental results. The deviations between theory and experiment are of the order of 10 %, which is somewhat more although of the same order of magnitude as the experimental uncertainty. It remains to be seen whether a refinement of the theory and of the experimental accuracy will remove the discrepancies.

We wish to thank Professor NIELS BOHR for the excellent working conditions at his Institute. Essential help was received in the form of seven sources from Dr. E. P. STEINBERG of the Argonne National Laboratory, and two isotope separations by ing. O. SKILBREID. Most of the chemical mani-

pulations were ably performed by Mrs. HELLE NORDBY. We thank E. SKURNIK and B. ELBEK for supplying us with data in advance of publication. Valuable suggestions have been received from A. BOHR, T. HUUS, B. MOTTELSON, O. B. NIELSEN, and S. G. NILSSON.

Two of the authors (R. E. B. and J. C. S.) wish to thank the Institute for Theoretical Physics for its hospitality, and one (J. C. S.) wishes to thank the Ford Foundation for making his stay in Copenhagen possible.

Institute for Theoretical Physics, University of Copenhagen.
Radiation Laboratory, Department of Physics,
McGill University, Montreal.
Physics and Mathematics Branch, Division of Research,
U.S. Atomic Energy Commission, Washington 25, D.C.

References

(1) K. ALDER *et al.*, Revs. Mod. Phys. **28**, 432 (1956).
(2) R. E. GREEN and R. E. BELL, Nuclear Instruments **3**, 127 (1958).
(3) R. E. BELL and M. H. JØRGENSEN, Can. J. Phys. **38**, 652 (1960).
(4) D. STROMINGER, J. M. HOLLANDER, and G. F. SEABORG, Revs. Mod. Phys. **30**, 585 (1958).
(5) J. G. SIEKMAN and H. DE WAARD, Nuclear Physics **8**, 402 (1958).
(6) J. C. SEVERIENS and F. W. RICHTER, Nuclear Physics **13**, 239 (1959).
(7) H. VARTAPÉTIAN, Comptes Rend. **246**, 1846 (1958).
(8) J. G. SIEKMAN and G. T. POTT, Physica **25**, 179 (1959).
(9) H. VARTAPÉTIAN and R. FOUCHER, Comptes Rend. **246**, 939 (1958).
(10) K. O. NIELSEN and O. SKILBREID, Nuclear Instruments **2**, 15 (1958).
(11) E. SKURNIK, B. ELBEK, and M. C. OLESEN, private communication. See also reference (1).
(12) B. R. MOTTELSON and S. G. NILSSON, Mat. Fys. Skr. Dan. Vid. Selsk. **1**, no. 8 (1959).
(13) M. E. ROSE, Internal Conversion Coefficients, North-Holland Publishing Co., Amsterdam, 1958.
(14) B. ELBEK, M. C. OLESEN, and O. SKILBREID, Nuclear Physics (to be published).
(15) S. T. BELYAEV, Mat. Fys. Medd. Dan. Vid. Selsk. **31**, no. 11 (1959).

Indleveret til selskabet 16. marts 1960.
Færdig fra trykkeriet 31. oktober 1960.